Kent Academic Repository

Downloaded from

The version of record is available from

This document version
Pre-print

DOI for this version

Licence for this version
UNSPECIFIED

Additional information

Versions of research works

Quantum lump dynamics on the two-sphere

S. Krusch[*]

School of Mathematics, Statistics and Actuarial Science, University of Kent
Canterbury CT2 7NF, England

J.M. Speight[†]

School of Mathematics, University of Leeds
Leeds LS2 9JT, England

Abstract

It is well known that the low-energy classical dynamics of solitons of Bogomol'nyi type is well approximated by geodesic motion in M_n, the moduli space of static n-solitons. There is an obvious quantization of this dynamics wherein the wavefunction $\psi : \mathsf{M}_n \to \mathbb{C}$ evolves according to the Hamiltonian $H_0 = \frac{1}{2}\triangle$, where $\triangle$ is the Laplacian on M_n. Born-Oppenheimer reduction of analogous mechanical systems suggests, however, that this simple Hamiltonian should receive corrections including κ, the scalar curvature of M_n, and $\mathscr{C}$, the n-soliton Casimir energy, which are usually difficult or impossible to compute, and whose effect on the energy spectrum is unknown. This paper analyzes the spectra of H_0 and two corrections to it suggested by work of Moss and Shiiki, namely $H_1 = H_0 + \frac{1}{4}\kappa$ and $H_2 = H_1 + \mathscr{C}$, in the simple but nontrivial case of a single $\mathbb{C}P^1$ lump moving on the two-sphere. Here $\mathsf{M}_1 = \mathsf{Rat}_1$, a noncompact kähler 6-manifold invariant under an $SO(3) \times SO(3)$ action, whose geometry is well understood. The symmetry gives rise to two conserved angular momenta, spin and isospin. By exploiting the diffeomorphism $\mathsf{Rat}_1 \cong TSO(3)$, a hidden isometry of Rat_1 is found which implies that all three energy spectra are symmetric under spin-isospin interchange. The Casimir energy is found exactly on a $SO(3)$ submanifold of Rat_1, using standard results from harmonic map theory and zeta function regularization, and approximated numerically on the rest of Rat_1. The lowest 19 eigenvalues of H_i are found, and their spin-isospin and parity compared for $i = 0, 1, 2$. It is found that the curvature corrections in H_1 lead to a qualitatively unchanged low-level spectrum while the Casimir energy in H_2 leads to significant changes. The scaling behaviour of the spectra under changes in the radii of the domain and target spheres is analyzed, and it is found that the disparity between the spectra of H_1 and H_2 is reduced when the target sphere is made smaller.

[*]E-mail: `S.Krusch@kent.ac.uk`
[†]E-mail: `speight@maths.leeds.ac.uk`

1 Introduction

Many field theories arising naturally in theoretical high energy physics may be said to be of Bogomol'nyi type. For such theories there is a topological lower bound on the energy of field configurations, and this bound is attained only by solutions of a first order "self-duality" equation, the so-called solitons of the theory. The solitons are stable by virtue of their energy-minimizing property, and are generically spatially localized lumps of energy with strongly particle-like characteristics. Examples are magnetic monopoles, abelian Higgs vortices and sigma model lumps. There is a well-developed geometric framework for studying the classical low-energy dynamics of such solitons, proposed originally for monopoles by Manton [22], called the geodesic approximation. Here, n-soliton trajectories are approximated by geodesics in the moduli space M_n of static n-solitons, with respect to the metric induced by the kinetic energy functional of the field theory (usually called the L^2 metric). This approach has been extremely fruitful, providing both important qualitative insight into topological soliton dynamics and good agreement with numerical analysis of the full field theory. In the case of vortices and monopoles, the geodesic approximation is backed by rigorous analysis [38, 39]. For a comprehensive review, see [23].

When one comes to quantize the low-energy dynamics of such solitons, two approaches are possible. Since geodesic motion on M_n captures the classical soliton dynamics so well, it is natural simply to quantize that [13]. Then the quantum n-soliton state is specified by a wavefunction $\psi : \mathsf{M}_n \to \mathbb{C}$, evolving subject to the Hamiltonian

$$H_{geo} = \tfrac{1}{2}\triangle, \tag{1.1}$$

where $\triangle$ is the Hodge Laplacian on M_n. This has the virtue of simplicity, but it ignores the degrees of freedom normal to the moduli space completely. An alternative is to make a low energy reduction of the full quantum field theory by means of the Born-Oppenheimer approximation. This has been carried out for sigma model lumps by Moss and Shiiki [28]. Arguing by analogy with finite dimensional mechanical systems, they find that, once again, the low energy quantum dynamics of n solitons can be described by a wavefunction on M_n, but that the Hamiltonian is

$$H_{BO} = \tfrac{1}{2}\triangle + \tfrac{1}{4}\kappa - \tfrac{1}{8}\|\boldsymbol{k}\|^2 + U + \cdots, \tag{1.2}$$

where κ is the scalar curvature of M_n, $\boldsymbol{k}$ is the mean curvature of the embedding of M_n into the (infinite dimensional) field configuration space and U is a potential on M_n incorporating the residual effects of the normal modes. This potential is rather complicated, but its dominant term is the n-soliton Casimir energy, that is, the total zero-point energy of the normal modes to the static n-soliton.

The aim of the current paper is to compare the spectra of H_{geo} and H_{BO}, to determine to what extent the extra terms in (1.2) change the quantum energy spectrum. Of course, one expects the numerical values of the energy eigenvalues to change to some extent. In itself, this is not particularly important. We will be more interested in the *qualitative* features of the energy spectrum. For example, on a noncompact moduli space, one could easily imagine that H_{geo} may have no bound states, while H_{BO} does. In the extreme case, one could find

that the spectrum of H_{geo} is continuous while that of H_{BO} is discrete. Clearly, H_{geo} would be a disastrously bad approximation in this case. Other, more refined, qualitative features can also be compared, for example, the dimension and symmetry properties of the eigenspaces of H_{geo} and H_{BO}, ordered by energy.

We address this issue for a specific example, namely a single $\mathbb{C}P^1$ lump moving on the two sphere (spacetime $S^2 \times \mathbb{R}$). This choice has several mathematical advantages, making it simple enough to be tractable, but not too simple to provide a nontrivial test of the truncation H_{geo}. First, the static n-solitons are explicitly known – they are rational maps, so $\mathsf{M}_n = \mathsf{Rat}_n$. Second, by choosing physical space to be compact (S^2 here) rather than $\mathbb{R}^2$ (as for the model on Minkowski space $\mathbb{R}^{2+1}$), we ensure that the L^2 metric on Rat_n is well defined (there are no non-normalizable zero modes). Third, we may think of the L^2 metric (formally) as the induced metric on Rat_n as a complex submanifold of $(\mathbb{C}P^1)^{S^2}$, the infinite dimensional space of maps $S^2 \to \mathbb{C}P^1$. This latter is (formally) an infinite product of kähler manifolds, so is kähler, so, as noted by Moss and Shiiki [28], the very awkward extrinsic curvature term is absent, $\|\boldsymbol{k}\|^2 = 0$. Fourth, the L^2 metric on Rat_1 is highly symmetric, so the L^2 metric and its scalar curvature can be computed explicitly. On the other hand, Rat_1 is not *too* symmetric: the scalar curvature and Casimir energy are non-constant functions of a single variable, the lump width, so that (in contrast to the case of monopoles and vortices) even the $n = 1$ sector provides a nontrivial test.

To be precise, we will compute the spectra of three approximations to H_{BO},

$$H_0 = H_{geo} = \tfrac{1}{2}\triangle, \qquad H_1 = \tfrac{1}{2}\triangle + \tfrac{1}{4}\kappa, \qquad H_2 = \tfrac{1}{2}\triangle + \tfrac{1}{4}\kappa + \mathscr{C}, \qquad (1.3)$$

where $\mathscr{C}$ is the Casimir energy. We will find that the spectrum of H_0 can be thought of as a perturbed version of the spectrum of the Laplacian on $\mathbb{C}P^3$ (equipped with the Fubini-Study metric). Quantum lumps possess two integer conserved angular momentum quantum numbers, which we call isospin k and spin t, associated with the rotational symmetries of the target space $\mathbb{C}P^1$ and the domain S^2 respectively. We will show that for each choice of k, t, the spectral problem for H_i, $i = 0, 1, 2$, reduces to a matrix Sturm-Liouville problem of dimension $2\min\{k, t\} + 1$. We find that this problem is symmetric under interchange of k and t, so the energy spectra of H_0, H_1, H_2 all possess this symmetry. A careful analysis of the boundary conditions for the Sturm-Liouville problem shows that the boundary conditions appropriate for H_1 are the same as for H_2, but different from H_0: including scalar curvature changes the boundary conditions. Nonetheless, the spectrum is discrete in all three cases. We have computed (numerically) the first 19 energy eigenvalues for each Hamiltonian and tabulated $\{k, t\}$ for the eigenstates in order of increasing energy. The spectra of H_0 and H_1 are remarkably similar. The order of states is the same apart from two transpositions. The Casimir energy leads to significant changes in the spectrum. However, the effect of the Casimir energy becomes less important if the radius of the target space is decreased.

2   The one-lump moduli space

Identifying $\mathbb{C}P^1 \cong S^2$ and using complex stereographic coordinates $z = x + iy$ and W on domain and codomain respectively, we may identify a map $\phi : S^2 \to \mathbb{C}P^1 \cong S^2$ with a

complex function $W(z)$. The kinetic and potential energy functionals of the $\mathbb{C}P^1$ model on S^2 are then

$$T = \frac{1}{2} \int \frac{4|W_t|^2}{(1+|W|^2)^2} \frac{4\mathrm{d}x\mathrm{d}y}{(1+|z|^2)^2}, \qquad V = \frac{1}{2} \int \frac{4(|W_x|^2 + |W_y|^2)}{(1+|W|^2)^2} \mathrm{d}x\mathrm{d}y \tag{2.1}$$

respectively. Note that, in contrast with earlier work [3, 25, 36, 37] we have given both domain and codomain spheres the round metric of radius 1. This will allow us to make direct use of results in the harmonic maps literature when we come to compute the Casimir energy of a lump. We will consider how our results change when the radii of the domain and target spheres are altered in section 5.5.

A theorem of Lichnerowicz [20] shows that, if ϕ has topological degree n (assumed, without loss of generality, to be non-negative), then $V \geq 4\pi n$, with equality if and only if ϕ is holomorphic. So degree n holomorphic maps $\phi : S^2 \to S^2$ minimize V within their homotopy class: these are the solitons of the model, and the "self-duality" equation is the Cauchy-Riemann equation. In terms of W and z, degree n holomorphic maps $S^2 \to S^2$ are rational maps of (algebraic) degree n, that is,

$$W = \frac{a_1 z^n + \cdots + a_{n+1}}{a_{n+2} z^n + \cdots + a_{2n+2}}, \tag{2.2}$$

where a_i are $2n+2$ complex constants, a_1 and a_{n+2} do not both vanish, and the numerator and denominator have no common roots. One interprets this physically as a static superposition of n lumps. So the moduli space of static n-lumps is Rat_n, the space of degree n rational maps.

The L^2 metric on Rat_n is defined by restricting the kinetic energy functional T to fields $W(t, z)$ which at each fixed t are degree n rational maps. Explicitly, in the chart where $a_1 \neq 0$, one can define local complex coordinates $q_i = a_i/a_1$, $i = 2, \ldots, 2n+2$ on Rat_n. Then allowing $q_2, \ldots, q_{2n+2}$ to vary with time, one substitutes

$$W(t, z) = \frac{z^n + q_2(t) z^{n-1} + \cdots + q_{n+1}(t)}{q_{n+2}(t) z^n + q_{n+3}(t) z^{n-1} + \cdots + q_{2n+2}(t)} \tag{2.3}$$

into T, to obtain

$$T = \frac{1}{2} \sum_{ij} \gamma_{ij} \dot{q}_i \overline{\dot{q}_j}, \qquad \gamma_{ij} = \int \frac{4}{(1+|W|^2)^2} \frac{\partial W}{\partial q_i} \frac{\overline{\partial W}}{\partial q_j} \frac{4\mathrm{d}x\mathrm{d}y}{(1+|z|^2)^2}. \tag{2.4}$$

The L^2 metric is $\gamma = \sum_{i,j} \gamma_{ij} \mathrm{d}q_i \mathrm{d}\overline{q}_j$. See [37] for a coordinate free definition of γ. The metric γ is manifestly Hermitian. In fact, it is kähler [32, 37]. It is known to be geodesically incomplete [33], so the classical geodesic approximation predicts lumps may collapse to infinitely narrow spikes in finite time. Numerical simulation and rigorous analysis (albeit on domain $\mathbb{C}$) confirm that lump collapse can occur, though the geodesic approximation gets the fine detail of the singularity formation process wrong [7, 21, 31].

There is an isometric action of $G = SO(3) \times SO(3)$ on Rat_n, induced by the natural $SO(3)$ actions on the domain and target spheres. On Rat_1 this action has cohomogeneity 1 (generic G orbits have codimension 1), and, in fact, almost completely determines γ. Consequently, an explicit formula for γ is known in this case, and the geometry is particularly well understood.

For $n = 1$, the no common roots condition on the rational map $W(z) = (a_1 z + a_2)/(a_3 z + a_4)$ is $a_1 a_4 - a_2 a_3 \neq 0$, so we may identify each map with a projective equivalence class $[L]$ of $GL(2, \mathbb{C})$ matrices,

$$\frac{a_1 z + a_2}{a_3 z + a_4} \leftrightarrow \left[\begin{pmatrix} a_1 & a_2 \\ a_3 & a_4 \end{pmatrix} \right]. \tag{2.5}$$

Hence $\mathsf{Rat}_1 \cong PL(2, \mathbb{C})$. The action of G on Rat_1 corresponds, under this identification, with the natural action of $PU(2) \times PU(2)$ on $PL(2, \mathbb{C})$:

$$([U_1], [U_2]) : [L] \mapsto [U_1 L U_2^{-1}]. \tag{2.6}$$

Now every $[L] \in PL(2, \mathbb{C})$ has a unique polar decomposition

$$[L] = [U(\Lambda \mathbb{I}_2 + \boldsymbol{\lambda} \cdot \boldsymbol{\tau})], \tag{2.7}$$

where $([U], \boldsymbol{\lambda}) \in PU(2) \times \mathbb{R}^3$, $\Lambda = \sqrt{1 + \lambda^2}$, $\lambda = |\boldsymbol{\lambda}|$, and τ_1, τ_2, τ_3 are the Pauli spin matrices. Hence $\mathsf{Rat}_1 \cong PU(2) \times \mathbb{R}^3$. Having chosen a basis $\{\frac{i}{2}\tau_a\}$ for $\mathfrak{su}(2)$, we have a canonical identification $PU(2) \cong SO(3)$ under which $[U]$ is identified with the orthogonal transformation $Ad_U : \mathfrak{su}(2) \to \mathfrak{su}(2)$. Hence $\mathsf{Rat}_1 \cong SO(3) \times \mathbb{R}^3$, and the G action is

$$(R_1, R_2) : (R, \boldsymbol{\lambda}) \mapsto (R_1 R R_2^{-1}, R_2 \boldsymbol{\lambda}). \tag{2.8}$$

From this we see that the G-orbits are level sets of λ, generically diffeomorphic to $SO(3) \times S^2$ (when $\lambda > 0$), the only exception being $\lambda = 0$, which is diffeomorphic to $SO(3)$. Physically, the lump corresponding to $(R, \boldsymbol{\lambda}) \in SO(3) \times \mathbb{R}^3$ has maximum energy density at $-\boldsymbol{\lambda}/\lambda \in S^2$, sharpness proportional to λ and internal orientation R. The $\lambda = 0$ lumps have uniform energy density.

The following explicit characterization of G invariant kähler metrics on Rat_1 was established in [37] (see [3] for an alternative viewpoint, exploiting more directly the covering $SL(2, \mathbb{C}) \to \mathsf{Rat}_1$):

Proposition 1 *Let γ be a $SO(3) \times SO(3)$ invariant kähler metric on Rat_1. Then*

$$\gamma = A_1 \, d\boldsymbol{\lambda} \cdot d\boldsymbol{\lambda} + A_2 (\boldsymbol{\lambda} \cdot d\boldsymbol{\lambda})^2 + A_3 \, \boldsymbol{\sigma} \cdot \boldsymbol{\sigma} + A_4 (\boldsymbol{\lambda} \cdot \boldsymbol{\sigma})^2 + A_1 \boldsymbol{\lambda} \cdot (\boldsymbol{\sigma} \times d\boldsymbol{\lambda}), \tag{2.9}$$

where $A_1, \ldots, A_4$ are smooth functions of λ only, all determined from the single function $A_1 = A(\lambda)$ by the relations

$$A_2 = \frac{A(\lambda)}{1 + \lambda^2} + \frac{A'(\lambda)}{\lambda}, \quad A_3 = \frac{1}{4}(1 + 2\lambda^2) A(\lambda), \quad A_4 = \frac{1}{4\lambda}(1 + \lambda^2) A'(\lambda). \tag{2.10}$$

Here $\sigma_1, \sigma_2, \sigma_3$ are the left invariant one forms on $SO(3)$ dual to the basis $\{\frac{i}{2}\tau_a : a = 1, 2, 3\}$ for $\mathfrak{su}(2) \cong \mathfrak{so}(3)$, $\times$ and $\cdot$ denote the vector and scalar product on $\mathbb{R}^3$ respectively and juxtaposition of one-forms denotes symmetrized tensor product.

So symmetries and the kähler property determine the metric up to a single function $A(\lambda)$, which we may think of as the squared length of the vector $\partial/\partial \lambda_1$ at the point $(\mathbb{I}_3, (0, 0, \lambda)) \in SO(3) \times \mathbb{R}^3$, corresponding to the rational map

$$W(z) = \mu z, \qquad \mu = \frac{\Lambda + \lambda}{\Lambda - \lambda}. \tag{2.11}$$

5

For the L^2 metric, one finds that

$$A = \frac{32\pi\mu[\mu^4 - 4\mu^2 \log\mu - 1]}{(\mu^2 - 1)^3}.$$ (2.12)

It follows from these formulae that (Rat_1, γ) has finite diameter and volume ($16^3\pi^6/6$ according to Baptista [3]), is Ricci positive and has unbounded scalar and holomorphic sectional curvatures. Examining the large λ behaviour of γ, one finds that the boundary at infinity of Rat_1 is $S^2 \times S^2$. Geodesic flow in (Rat_1, γ) was studied in detail in [36, 14], and turns out to be surprisingly complicated given the homogeneity and isotropy of physical space. In particular, lumps generically do not travel along great circles in S^2.

It is important to realize that *any* kähler metric on Rat_1 invariant under the $SO(3) \times SO(3)$ action must have the structure of Proposition 1 for some function $A(\lambda)$. There is one other natural metric on Rat_1 which we will have reason to consider. By identifying a rational map with the projective equivalence class of its coefficients, we may think of Rat_1 as an open subset of $\mathbb{C}P^3$,

$$\mathsf{Rat}_1 \hookrightarrow \mathbb{C}P^3, \qquad \frac{a_1 z + a_2}{a_3 z + a_4} \mapsto [a_1, a_2, a_3, a_4].$$ (2.13)

We equip $\mathbb{C}P^3$ with the Fubini-Study metric of constant holomorphic sectional curvature 4, whence Rat_1 inherits a kähler metric, which we shall also call the Fubini-Study metric γ_{FS}. It is not hard to show [37] that γ_{FS} is $SO(3) \times SO(3)$ invariant, and so has the structure of Proposition 1. One finds that the coefficient function is

$$A_{FS} = \frac{2\mu}{1 + \mu^2} = \frac{1}{2\lambda^2 + 1}.$$ (2.14)

Finally, given any $SO(3) \times SO(3)$ invariant kähler metric on Rat_1, it is convenient to define a second metric coefficient function, the squared length at $([\mathbb{I}_2], (0, 0, \lambda))$ of θ_3, where $\theta_1, \theta_2, \theta_3$ are the left-invariant vector fields on $SO(3)$ dual to $\sigma_1, \sigma_2, \sigma_3$. This turns out to be

$$B = \frac{1}{4}(\lambda^2 + \Lambda^2)A + \frac{1}{4}\lambda\Lambda^2 A'.$$ (2.15)

For the L^2 and Fubini-Study metrics one finds, respectively,

$$\begin{aligned}
B &= \frac{32\pi\mu^2}{(\mu^2 - 1)^3}[(\mu^2 + 1)\log\mu - \mu^2 + 1], \\
B_{FS} &= \frac{1}{4(\lambda^2 + \Lambda^2)^2} = \frac{1}{4(2\lambda^2 + 1)^2}.
\end{aligned}$$ (2.16)

3 The Laplacian on Rat_1

We begin the computation of the Laplacian on functions on Rat_1 by proving a lemma which generalizes the well-known expression for $\triangle$ in local coordinates.

Lemma 2 *Let (M^m, g) be a Riemannian manifold of dimension m, $\{X_i\}$ be a local frame on M, $\{\nu_i\}$ be the associated coframe, and $\{\mu_i\}$ be the associated basis for $\Lambda^{m-1}M$, that is,*

$$\mu_1 = \nu_2 \wedge \nu_3 \wedge \cdots \wedge \nu_m, \quad \mu_2 = \nu_1 \wedge \nu_3 \wedge \cdots \wedge \nu_m, \quad \cdots, \quad \mu_m = \nu_1 \wedge \nu_2 \wedge \cdots \wedge \nu_{m-1}.$$

If all the $(m-1)$-forms μ_i are closed, then the Laplacian on functions is

$$\triangle f = -\frac{1}{\sqrt{|g|}} \sum_{i,j} X_i[\sqrt{|g|}\widehat{g}(\nu_i, \nu_j) X_j[f]],$$

where $\widehat{g}$ is the inverse metric and $|g| = \det(g_{..})$.

Proof: We use the summation convention on repeated indices, and define $g^{ij} = \widehat{g}(\nu_i, \nu_j)$. The Laplacian on functions is $\triangle = -*\mathrm{d}*\mathrm{d}$, where $*$ denotes the Hodge isomorphism, so

$$\begin{aligned}
\triangle f &= -*\mathrm{d}(X_i[f]*\nu_i) = -*\mathrm{d}(X_i[f]\frac{\sqrt{|g|}}{(m-1)!}g^{ij}\epsilon_{ji_2i_3\cdots i_m}\nu_{i_2}\wedge\cdots\wedge\nu_{i_m})\\
&= -*X_k[X_i[f]\sqrt{|g|}g^{ij}]\frac{\epsilon_{ji_2i_3\cdots i_m}}{(m-1)!}\nu_k\wedge\nu_{i_2}\wedge\cdots\wedge\nu_{i_m}\\
&= -*X_j[X_i[f]\sqrt{|g|}g^{ij}]\nu_1\wedge\nu_2\wedge\cdots\wedge\nu_m,
\end{aligned}$$

where we have used $\mathrm{d}(\nu_{i_2}\wedge\cdots\wedge\nu_{i_m}) = 0$. Now the volume form is $\mathrm{vol} = \sqrt{|g|}\nu_1\wedge\cdots\wedge\nu_m$ and $*\mathrm{vol} = 1$, so

$$\triangle f = -X_j[X_i[f]\sqrt{|g|}g^{ij}]\frac{1}{\sqrt{|g|}}$$

as claimed. $\square$

Note that any local coordinate basis $X_i = \partial/\partial x^i$ satisfies the conditions automatically, and that the formula for $\triangle$ reduces to the usual expression in this case. For our purposes it is convenient to use the (global) frame $\{\partial_a, \theta_a : a = 1, 2, 3\}$ on Rat_1, where $\partial_a = \partial/\partial\lambda_a$ and θ_a are the left-invariant vector fields on $SO(3)$ dual to σ_a. We thus require an expression for the inverse metric $\widehat{\gamma}$ relative to this frame.

Proposition 3 *Let γ be a $SO(3) \times SO(3)$ invariant kähler metric on Rat_1 determined, as in Proposition 1, by the function $A(\lambda)$. Then the inverse metric $\widehat{\gamma}$ is*

$$\widehat{\gamma} = C_1\boldsymbol{\partial}\cdot\boldsymbol{\partial} + C_2(\boldsymbol{\lambda}\cdot\boldsymbol{\partial})^2 + C_3\boldsymbol{\theta}\cdot\boldsymbol{\theta} + C_4(\boldsymbol{\lambda}\cdot\boldsymbol{\theta})^2 + C_5\boldsymbol{\lambda}\cdot(\boldsymbol{\theta}\times\boldsymbol{\partial}) \tag{3.1}$$

where $C_1, \ldots, C_5$ are smooth functions of λ alone satisfying

$$C_1 = \frac{\Lambda^2 + \lambda^2}{\Lambda^2 A}, \quad C_1 + \lambda^2 C_2 = \frac{\Lambda^2}{4B}, \quad C_3 = \frac{4}{\Lambda^2 A}, \quad C_3 + \lambda^2 C_4 = \frac{1}{B}, \quad C_5 = C_3.$$

Here $\boldsymbol{\partial} = (\partial/\partial\lambda_1, \partial/\partial\lambda_2, \partial/\partial\lambda_3)$, $\boldsymbol{\theta} = (\theta_1, \theta_2, \theta_3)$, juxtaposition of vector fields denotes symmetrized tensor product, and B is determined by A as in equation (2.15).

7

Proof: The same symmetry argument used to prove Proposition 1 (Proposition 3.1 of [37]) shows that every invariant symmetric $(2,0)$ tensor is of the above form, with $C_1, \ldots, C_5$ some functions of λ only. The formulae for $C_1, \ldots, C_5$ result from explicit computation of $\|d\lambda_a\|^2$, $\|\sigma_a\|^2$ and $\langle d\lambda_a, \sigma_b \rangle$ $a, b = 1, 2, 3$, at the point $([\mathbb{I}], (0, 0, \lambda))$ for general λ, using the unitary frame $\{e_a, Je_a : a = 1, 2, 3\}$ introduced in section 4.1 of [37]. For example, at $([\mathbb{I}], (0, 0, \lambda))$,

$$\|\sigma_3\|^2 = C_3 + \lambda^2 C_4 = \sum_{a=1}^{3}(\sigma_3(e_a)^2 + \sigma_3(Je_a)^2) = \sigma_3(Je_3)^2 = \frac{1}{B}.$$

$\square$

Proposition 4 *Let γ be a $SO(3) \times SO(3)$ invariant kähler metric on Rat_1 determined as in Proposition 1 by the function $A(\lambda)$. Then the Laplacian on (Rat_1, γ) is*

$$
\begin{aligned}
\triangle f &= -\frac{4}{\Lambda^2 A}\left\{\boldsymbol{\theta} \cdot \boldsymbol{\theta} f + \boldsymbol{\lambda} \cdot (\boldsymbol{\partial} \times \boldsymbol{\theta})f - \frac{1}{\lambda^2}\left[1 - \frac{\Lambda^2 A}{4B}\right](\boldsymbol{\lambda} \cdot \boldsymbol{\theta})^2 f\right\} \\
&\quad - \frac{1}{\Lambda\lambda^2 A^2 B}\frac{\partial}{\partial\lambda}\left(\frac{\lambda^2 \Lambda^3 A^2}{4}\frac{\partial f}{\partial\lambda}\right) - \frac{\Lambda^2 + \lambda^2}{\lambda^2\Lambda^2 A}(\boldsymbol{\lambda} \times \boldsymbol{\partial}) \cdot (\boldsymbol{\lambda} \times \boldsymbol{\partial})f.
\end{aligned}
\tag{3.2}
$$

Proof: We work with the frame $\{\partial_a, \theta_a : a = 1, 2, 3\}$. Note that $d(d\lambda_a) = 0$ and

$$d\sigma_1 = \sigma_2 \wedge \sigma_3, \quad d\sigma_2 = \sigma_3 \wedge \sigma_1, \quad d\sigma_3 = \sigma_1 \wedge \sigma_2,$$

so any wedge product of five of these one forms is closed. Hence this frame satisfies the conditions of Lemma 2 which, with Proposition 3, immediately gives

$$
\begin{aligned}
\triangle f &= -\frac{1}{\sqrt{|\gamma|}}\left\{\boldsymbol{\partial} \cdot (\sqrt{|\gamma|}(C_1\boldsymbol{\partial} f + C_2\boldsymbol{\lambda}(\boldsymbol{\lambda} \cdot \boldsymbol{\partial}[f]))) + \boldsymbol{\partial} \cdot (-\sqrt{|\gamma|}\frac{C_5}{2}\boldsymbol{\lambda} \times \boldsymbol{\theta}[f])\right. \\
&\quad \left. + \boldsymbol{\theta} \cdot (\sqrt{|\gamma|}\frac{C_5}{2}\boldsymbol{\lambda} \times \boldsymbol{\partial}[f]) + \boldsymbol{\theta} \cdot (\sqrt{|\gamma|}(C_3\boldsymbol{\theta}[f] + C_4\boldsymbol{\lambda}(\boldsymbol{\lambda} \cdot \boldsymbol{\theta}[f])))\right\}.
\end{aligned}
\tag{3.3}
$$

Now the volume form on (Rat_1, γ) is [37]

$$\text{vol} = \frac{\Lambda}{2}A^2 B d\lambda_1 \wedge d\lambda_2 \wedge d\lambda_3 \wedge \sigma_1 \wedge \sigma_2 \wedge \sigma_3,
\tag{3.4}$$

whence one sees that $\sqrt{|\gamma|} = \frac{\Lambda}{2}A^2 B$ for this frame. Substituting this, and the formulae for $C_1, \ldots, C_5$ (Proposition 3) into equation (3.3) yields, after some straightforward manipulation, the formula claimed. $\square$

As a check on our formula, we should verify that it is consistent with the $SO(3) \times SO(3)$ symmetry of γ. That is, the operator $\triangle$ must commute with all Killing vector fields on (Rat_1, γ). There are six independent Killing vector fields on (Rat_1, γ), three generating the left $SO(3)$ action and three generating the right $SO(3)$ action. Recall that the left action on $\mathsf{Rat}_1 \cong SO(3) \times \mathbb{R}^3$ acts by left translation on $SO(3)$ and acts trivially on $\mathbb{R}^3$. Now left

8

translations on a Lie group are generated by *right* invariant vector fields. So, let ξ_a, $a = 1, 2, 3$, be the right invariant vector fields on $SO(3)$ coinciding at $\mathbb{I}$ with θ_a. Since the left and right actions commute, $[\theta_a, \xi_b] = 0$ for all a, b so we see immediately that $\triangle$ as in formula (3.2) commutes with each ξ_a. The right action of $SO(3)$ on $\mathsf{Rat}_1 \cong SO(3) \times \mathbb{R}^3$ acts by right translation on $SO(3)$ and by the fundamental representation on $\mathbb{R}^3$. Hence the Killing vector fields generating this action are $X_a = \theta_a + \Phi_a$ where $\Phi_a = \epsilon_{abc}\lambda_b\partial_c$. Note that $\{\theta_a\}$, $\{\Phi_a\}$ and $\{X_a\}$ each satisfy the angular momentum algebra,

$$[\theta_a, \theta_b] = -\epsilon_{abc}\theta_c, \quad [\Phi_a, \Phi_b] = -\epsilon_{abc}\Phi_c, \quad [X_a, X_b] = -\epsilon_{abc}X_c, \tag{3.5}$$

and that $[\theta_a, \Phi_b] = 0$, so

$$[X_a, \boldsymbol{X} \cdot \boldsymbol{X}] = [X_a, \boldsymbol{\theta} \cdot \boldsymbol{\theta}] = [X_a, \boldsymbol{\Phi} \cdot \boldsymbol{\Phi}] = 0. \tag{3.6}$$

Clearly all these vector fields annihilate functions of λ and commute with $\partial/\partial\lambda$. It follows that X_a commutes with the first, fourth and fifth terms of (3.2). To deal with the second term, note that

$$[X_a, \boldsymbol{\lambda} \cdot (\boldsymbol{\partial} \times \boldsymbol{\theta})] = [X_a, \boldsymbol{\theta} \cdot \boldsymbol{\Phi}] = \frac{1}{2}[X_a, \boldsymbol{X} \cdot \boldsymbol{X} - \boldsymbol{\theta} \cdot \boldsymbol{\theta} - \boldsymbol{\Phi} \cdot \boldsymbol{\Phi}] = 0. \tag{3.7}$$

Finally, X_a commutes with the third term since

$$[X_a, \boldsymbol{\lambda} \cdot \boldsymbol{\theta}] = [\theta_a + \epsilon_{abc}\lambda_b\partial_c, \lambda_d\theta_d] = \lambda_d(-\epsilon_{ade}\theta_e) + \epsilon_{abd}\lambda_b\theta_d = 0. \tag{3.8}$$

4   Casimir energy

The dominant term in Moss and Shiiki's Hamiltonian arising from the degrees of freedom orthogonal to the moduli space is the Casimir energy $\mathscr{C}$, which is formally given by

$$\mathscr{C} = \frac{1}{2}\sum_i \omega_i, \tag{4.1}$$

where ω_i are the frequencies of oscillation of the normal modes of the static solution. In the field theory context, the above sum is infinite and divergent, so we must regularize it in some way. We return to this issue below. First we set about computing the frequencies ω_i in the case of interest, a single $\mathbb{C}P^1$ lump on S^2. To achieve this, we will make use of some standard results in the stability theory of harmonic maps, which we begin by briefly reviewing. This material is treated in detail in [40, ch. 5].

4.1   The spectrum of the Jacobi operator

Recall that given a map $\varphi : (M, g) \to (N, h)$ between Riemannian manifolds, its Dirichlet energy is

$$E = \frac{1}{2}\int_M \|\mathrm{d}\varphi\|^2, \tag{4.2}$$

and the map is harmonic if it is a critical point of E. This is directly relevant to us since, with the choice $(M, g) = (N, h) =$ the round sphere of radius 1, E coincides precisely with V, the $\mathbb{C}P^1$ model's potential energy functional. Hence, $\mathbb{C}P^1$ lumps are harmonic maps $S^2 \to S^2$. Given a harmonic map $\varphi : M \to N$, one defines its Hessian, a symmetric bilinear form on $\Gamma(\varphi^{-1}TN)$ (the space of smooth sections of the vector bundle over M whose fibre over $p \in M$ is the tangent space $T_{\varphi(p)}N$), as follows. Let $\varphi_{s,t} : M \to N$ be a smooth two-parameter variation of φ (so $\varphi_{0,0} = \varphi$), with $\partial_s \varphi_{s,t}|_{s=t=0} = X$, $\partial_t \varphi_{s,t}|_{s=t=0} = Y \in \Gamma(\varphi^{-1}TN)$. Then

$$\mathsf{Hess}_\varphi(X, Y) = \frac{\partial^2}{\partial s\, \partial t} E(\varphi_{s,t}) \Big|_{s=t=0}. \tag{4.3}$$

One says that φ is *stable* if $\mathsf{Hess}_\varphi(X, X) \geq 0$ for all X. Clearly, if φ minimizes E in its homotopy class, as in our case, it is stable.

Associated with Hess_φ, there is a self-adjoint, elliptic, linear differential operator $\mathscr{J}_\varphi : \Gamma(\varphi^{-1}TN) \to \Gamma(\varphi^{-1}TN)$, which is known as the Jacobi operator and is defined by

$$\mathsf{Hess}_\varphi(X, Y) = \langle X, \mathscr{J}_\varphi Y \rangle_{L^2} = \int_M h(X, \mathscr{J}_\varphi Y). \tag{4.4}$$

If M is compact, the harmonic map φ is stable if and only if the spectrum of $\mathscr{J}_\varphi$ is non-negative, and this spectrum is discrete, each eigenvalue having finite multiplicity. Any map $\psi : M \to N$ which is sufficiently close pointwise to a harmonic map φ can be uniquely written $\psi = \exp_\varphi X$, where $\|X\|$ is pointwise small, and then

$$E(\psi) = E(\varphi) + \frac{1}{2}\mathsf{Hess}_\varphi(X, X) + O(X^3) = E(\varphi) + \frac{1}{2}\langle X, \mathscr{J}_\varphi X \rangle_{L^2} + O(X^3), \tag{4.5}$$

whence it is clear that the eigenvalues of $\mathscr{J}_\varphi$ are precisely ω_i^2, the squared frequencies we require to compute $\mathscr{C}$.

There is an explicit formula for the Jacobi operator of a general harmonic map $\varphi : (M, g) \to (N, h)$,

$$\mathscr{J}_\varphi = \triangle_\varphi - \mathscr{R}_\varphi, \tag{4.6}$$

where $\triangle_\varphi$ is the rough Laplacian on $\Gamma(\varphi^{-1}TN)$, and $\mathscr{R}_\varphi$ is a certain section of $\mathrm{End}(\varphi^{-1}TN)$ constructed from the curvature tensor R^N on N. Explicitly, given a choice of local orthonormal frame $E_1, E_2, \ldots, E_m$ on M,

$$\triangle_\varphi Y = -\mathrm{tr}\,\nabla^\varphi \nabla^\varphi Y = -\sum_{i=1}^m \left\{ \nabla^\varphi_{E_i}(\nabla^\varphi_{E_i} Y) - \nabla^\varphi_{\nabla^M_{E_i} E_i} Y \right\}, \tag{4.7}$$

$$\mathscr{R}_\varphi Y = \sum_{i=1}^m R^N(Y, \mathrm{d}\varphi E_i)\mathrm{d}\varphi E_i, \tag{4.8}$$

where ∇^M, ∇^N are the Levi-Civita connexions of M, N respectively, and ∇^φ is the pullback to $\varphi^{-1}TN$ of ∇^N. In the case of interest to us, $\mathscr{R}_\varphi$ is somewhat easier to handle than $\triangle_\varphi$, owing to the following proposition:

Proposition 5 *Let $\varphi : (M^n, g) \to (N^n, h)$ be a weakly conformal mapping between Riemannian manifolds of equal dimension, and (N^n, h) be Einstein with scalar curvature κ (necessarily constant). Then*

$$\mathscr{R}_\varphi = \frac{2\kappa}{n^2} \mathcal{E} \operatorname{Id},$$

where $\mathcal{E} = \frac{1}{2}\|\mathrm{d}\varphi\|^2 \in C^\infty(M)$ is the Dirichlet energy density of φ.

Proof: Recall that φ is weakly conformal if there exists a smooth function $f : M \to \mathbb{R}$ such that $h(\mathrm{d}\varphi X, \mathrm{d}\varphi Y) = f^2 g(X, Y)$ for all vector fields X, Y on M. Let $E_1, \ldots, E_n$ be a local orthonormal frame on M. At all points $p \in M$ where $f(p) = 0$, $\mathrm{d}\varphi = 0$ so the desired equality holds trivially (both $\mathscr{R}_\varphi$ and $\mathcal{E}$ vanish). At all other points, $\|\mathrm{d}\varphi E_i\|^2 = \frac{2}{n}\mathcal{E} > 0$ independent of i and $h(\mathrm{d}\varphi E_i, \mathrm{d}\varphi E_j) = 0$ for $i \neq j$, so

$$\hat{E}_i = \sqrt{\frac{n}{2\mathcal{E}}} \mathrm{d}\varphi E_i, \qquad i = 1, 2, \ldots, n$$

form an orthonormal basis for $T_{\varphi(p)}N$. Hence, for all $X, Y \in T_{\varphi(p)}N$,

$$
\begin{aligned}
h(X, \mathscr{R}_\varphi Y) &= \sum_{i=1}^n h(X, R^N(Y, \mathrm{d}\varphi E_i)\mathrm{d}\varphi E_i) = \frac{2\mathcal{E}}{n} \sum_{i=1}^n h(X, R^N(Y, \hat{E}_i)\hat{E}_i) \\
&= -\frac{2\mathcal{E}}{n} \sum_{i=1}^n h(\hat{E}_i, R^N(Y, \hat{E}_i)X) = \frac{2\mathcal{E}}{n} \operatorname{Ric}(Y, X) = \frac{2\mathcal{E}}{n} \frac{\kappa}{n} h(X, Y) \quad (4.9)
\end{aligned}
$$

by a standard symmetry of R^N [41, p. 58] and the Einstein property of (N, h).   □

Note that every $\varphi \in \mathsf{Rat}_1$ is holomorphic, hence conformal, and the unit two-sphere is Einstein with $\kappa = 2$. Hence

$$\mathscr{R}_\varphi = \mathcal{E} \operatorname{Id} \tag{4.10}$$

in this case. Thinking of $\mathscr{J}_\varphi$ as a quantum Hamiltonian acting on "wavefunctions" on the two-sphere (sections of $\varphi^{-1}TN$, really), the effect of the curvature term is to add a potential well equal to minus the classical energy density of the lump. What is this energy density? By $SO(3) \times SO(3)$ invariance, the spectrum of $\mathscr{J}_\varphi$ can depend only on λ, so it suffices to consider only the one-parameter family of rational maps

$$\varphi : z \mapsto W = \mu(\lambda)z = \frac{\Lambda + \lambda}{\Lambda - \lambda} z \tag{4.11}$$

corresponding to the curve $([\mathbb{I}_2], (0, 0, \lambda))$, $\lambda \geq 0$, in $PU(2) \times \mathbb{R}^3$. It is convenient to parametrize these by $\mu \in [1, \infty)$ rather than $\lambda \in [0, \infty)$. In terms of the usual polar coordinates on both domain and codomain spheres, the map (4.11) is

$$\varphi : (\theta, \phi) \mapsto (f_\mu(\theta), \phi), \qquad \text{where} \quad f_\mu(\theta) = 2 \cot^{-1}\left(\mu \cot \frac{\theta}{2}\right). \tag{4.12}$$

The pair $E_1 = \partial/\partial\theta$, $E_2 = \operatorname{cosec}\theta\,\partial/\partial\phi$ is orthonormal on S^2, whence, by conformality, one sees that

$$\mathcal{E} = \|\mathrm{d}\varphi E_2\|^2 = \frac{\sin^2 f_\mu(\theta)}{\sin^2 \theta}. \tag{4.13}$$

11

We turn now to the explicit computation of the rough Laplacian $\triangle_\varphi$, for φ of the form (4.11). Note that $\widetilde{E}_1 = E_1 \circ \varphi$, $\widetilde{E}_2 = E_2 \circ \varphi$ gives an orthonormal pair of sections of $\varphi^{-1}TN$. Any section Y of $\varphi^{-1}TN$ can be uniquely written $Y = Y_1(\theta, \phi)\widetilde{E}_1 + Y_2(\theta, \phi)\widetilde{E}_2$. We seek an expression for $\triangle_\varphi$ as a differential operator acting on the pair of smooth functions (Y_1, Y_2). In fact, we can deduce all we need once we know how $\triangle_\varphi$ acts on sections of the form $a(\theta)\cos m\phi \widetilde{E}_1$ where $m \in \mathbb{N}$. A straightforward but lengthy computation, presented in the appendix, shows that

$$\triangle_\varphi(a(\theta)\cos m\phi \widetilde{E}_1) = (\mathscr{D}_m a)\cos m\phi \widetilde{E}_1 + Q_m a \sin m\phi \widetilde{E}_2 \tag{4.14}$$

$$\text{where} \quad \mathscr{D}_m = -\frac{d^2}{d\theta^2} - \cot\theta \frac{d}{d\theta} + \frac{m^2 + \cos^2 f_\mu}{\sin^2\theta} \tag{4.15}$$

$$Q_m = 2m\frac{\cos f_\mu}{\sin^2\theta}. \tag{4.16}$$

Since N is kähler, ∇^N commutes with J^N, the almost complex structure on N, namely $[\nabla^\varphi, J^N] = 0$, and hence $[\triangle_\varphi, J^N] = 0$ also. So we conclude immediately that

$$\triangle_\varphi(a(\theta)\cos m\phi \widetilde{E}_2) = \triangle_\varphi(J^N a(\theta)\cos m\phi \widetilde{E}_1) = J^N \triangle_\varphi(a(\theta)\cos m\phi \widetilde{E}_1)$$
$$= -Q_m a \sin m\phi \widetilde{E}_1 + (\mathscr{D}_m a)\cos m\phi \widetilde{E}_2. \tag{4.17}$$

Consider now the $SO(2)$ action on $C^\infty(S^2, S^2)$ given by

$$\varphi \mapsto \varphi_\alpha = R_\alpha \circ \varphi \circ R_{-\alpha} \quad \text{where} \quad R_\alpha = \begin{pmatrix} \cos\alpha & -\sin\alpha & 0 \\ \sin\alpha & \cos\alpha & 0 \\ 0 & 0 & 1 \end{pmatrix}, \quad \alpha \in \mathbb{R}. \tag{4.18}$$

Note that $E(\varphi_\alpha) \equiv E(\varphi)$ and each of the maps (4.11) is fixed under this $SO(2)$ action. It follows that $\mathscr{J}_\varphi$, and hence, by Proposition 5, $\triangle_\varphi$, commute with the induced action on $\Gamma(\varphi^{-1}TN)$,

$$Y \mapsto \mathsf{R}_\alpha(Y) = \mathrm{d}R_\alpha \circ Y \circ R_{-\alpha}, \tag{4.19}$$

or, in terms of polar coordinates,

$$\mathsf{R}_\alpha(Y_1(\theta, \phi)\widetilde{E}_1 + Y_2(\theta, \phi)\widetilde{E}_2) = Y_1(\theta, \phi - \alpha)\widetilde{E}_1 + Y_2(\theta, \phi - \alpha)\widetilde{E}_2. \tag{4.20}$$

Hence

$$\triangle_\varphi(a(\theta)\sin m\phi \widetilde{E}_2) = \triangle_\varphi(\mathsf{R}_{\frac{\pi}{2m}}a(\theta)\cos m\phi \widetilde{E}_2) = \mathsf{R}_{\frac{\pi}{2m}}\triangle_\varphi(a(\theta)\cos m\phi \widetilde{E}_2)$$
$$= \mathsf{R}_{\frac{\pi}{2m}}(-Q_m a \sin m\phi \widetilde{E}_1 + (\mathscr{D}_m a)\cos m\phi \widetilde{E}_2)$$
$$= Q_m a \cos m\phi \widetilde{E}_1 + (\mathscr{D}_m a)\sin m\phi \widetilde{E}_2, \tag{4.21}$$

and similarly

$$\triangle_\varphi(a(\theta)\sin m\phi \widetilde{E}_1) = (\mathscr{D}_m a)\sin m\phi \widetilde{E}_1 - Q_m a \cos m\phi \widetilde{E}_2. \tag{4.22}$$

To summarize, $\mathscr{J}_\varphi$ leaves each infinite dimensional subspace $I_m \subset \Gamma(\varphi^{-1}TN)$, $m \in \mathbb{N}$,

$$I_m = \{a_1(\theta)\cos m\phi \widetilde{E}_1 + a_2(\theta)\sin m\phi \widetilde{E}_2 + a_3(\theta)\cos m\phi \widetilde{E}_2 + a_4(\theta)\sin m\phi \widetilde{E}_1 : a \in C^\infty((0, \pi), \mathbb{R}^4)\} \tag{4.23}$$

12

invariant, these spaces span $\Gamma(\varphi^{-1}TN)$, and on I_m,

$$
\mathscr{J}_\varphi \begin{pmatrix} a_1 \\ a_2 \\ a_3 \\ a_4 \end{pmatrix} = \begin{pmatrix} \mathscr{D}_m - \mathcal{E} & Q_m & 0 & 0 \\ Q_m & \mathscr{D}_m - \mathcal{E} & 0 & 0 \\ 0 & 0 & \mathscr{D}_m - \mathcal{E} & -Q_m \\ 0 & 0 & -Q_m & \mathscr{D}_m - \mathcal{E} \end{pmatrix} \begin{pmatrix} a_1 \\ a_2 \\ a_3 \\ a_4 \end{pmatrix}.
\tag{4.24}
$$

This diagonalizes after a simple change of coordinates. Let $\alpha_1 = a_1 + a_2$, $\alpha_2 = a_3 + a_4$, $\alpha_3 = a_1 - a_2$ and $\alpha_4 = a_3 - a_4$. Then

$$
\mathscr{J}_\varphi \begin{pmatrix} \alpha_1 \\ \alpha_2 \\ \alpha_3 \\ \alpha_4 \end{pmatrix} = \begin{pmatrix} \mathscr{D}_m + Q_m - \mathcal{E} & 0 & 0 & 0 \\ 0 & \mathscr{D}_m + Q_m - \mathcal{E} & 0 & 0 \\ 0 & 0 & \mathscr{D}_m - Q_m - \mathcal{E} & 0 \\ 0 & 0 & 0 & \mathscr{D}_m - Q_m - \mathcal{E} \end{pmatrix} \begin{pmatrix} \alpha_1 \\ \alpha_2 \\ \alpha_3 \\ \alpha_4 \end{pmatrix}.
\tag{4.25}
$$

Note that $\mathscr{D}_{-m} = \mathscr{D}_m$ and $Q_{-m} = -Q_m$, so spec $\mathscr{J}_\varphi$ is the union of the spectra of the Sturm-Liouville operators

$$
S_m = \mathscr{D}_m + Q_m - \mathcal{E} = -\frac{d^2}{d\theta^2} - \cot\theta \frac{d}{d\theta} + U_m(\theta), \qquad m \in \mathbb{Z},
\tag{4.26}
$$

where

$$
U_m(\theta) = \frac{m^2 - 1 + 2\cos^2 f_\mu(\theta) + 2m\cos f_\mu(\theta)}{\sin^2 \theta}
\tag{4.27}
$$

and each eigenvalue occurs with double multiplicity. In terms of physics, we may think of this as the energy spectrum for "spin 0" (i.e. ϕ independent) states of a point particle moving on S^2 in the $SO(2)$ invariant potential well $U_m(\theta)$. The spectrum of each S_m may be computed numerically using the shooting method described in [14].

There is one value of μ for which spec $\mathscr{J}_\varphi$ may be computed exactly, namely $\mu = 1$. Here things simplify considerably, because the corresponding rational map is the identity map $S^2 \to S^2$. The Jacobi operator for the identity map on a general Riemannian manifold (M^n, g) was studied in detail by Smith [35]. The key simplification is that one has a canonical identification $\text{Id}^{-1}TN \equiv T^*M$, obtained by identifying the section Y of $\text{Id}^{-1}TN = TM$ with the one form $\flat Y = g(Y, \cdot)$. This is useful because there is a Weitzenböck formula relating the rough Laplacian $\triangle_{\text{Id}}$ to the Hodge Laplacian $\triangle$ on one-forms [40, p. 161]

$$
\triangle_{\text{Id}} Y = \sharp \left(\triangle \flat Y - \text{Ric}(Y, \cdot) \right).
\tag{4.28}
$$

In the case where M^n is Einstein, with (constant) scalar curvature κ,

$$
\sharp \, \text{Ric}(Y, \cdot) \equiv \frac{\kappa}{n} Y,
\tag{4.29}
$$

which together with Proposition 5 and the observation that $\mathcal{E} = \frac{n}{2}$, constant, for Id, gives the following formula for $\mathscr{J}_{\text{Id}}$ on an Einstein manifold, originally due to Smith,

$$
\mathscr{J}_{\text{Id}} = \sharp \triangle \flat - \frac{2\kappa}{n}.
\tag{4.30}
$$

13

In our case, $n = \kappa = 2$, so $\mathscr{J}_{\mathrm{Id}} = \sharp \triangle \flat - 2$, that is, the spectrum of $\mathscr{J}_\varphi$ in the special case $\mu = 1$ is the spectrum of the Hodge Laplacian on one-forms on S^2, shifted down by 2. This, in turn, can be related to the spectrum of the Laplacian on functions on S^2, as follows.

Let Ω_p denote the space of smooth p-forms on S^2, and $\delta : \Omega_p \to \Omega_{p-1}$ denote the coderivative, so that the Hodge Laplacian is $\triangle = \delta \mathrm{d} + \mathrm{d}\delta$. Every one-form on S^2 has a unique Hodge decomposition

$$Y_1 = \mathrm{d}Y_0 + \delta Y_2 \tag{4.31}$$

into exact and coexact components (the harmonic component vanishes as $H^1(S^2) = 0$). Now $\mathrm{d}\Omega_0$ and $\delta\Omega_2$ are L^2 orthogonal subspaces of Ω_1 and $[\triangle, \mathrm{d}] = [\triangle, \delta] = 0$, so the spectral problem for $\triangle_{\Omega_1}$ decomposes into two sub-problems, for $\triangle|_{\mathrm{d}\Omega_0}$ and $\triangle|_{\delta\Omega_2}$. Since Y_1 is coexact if and only if $*Y_1$ is exact, and $* : \Omega_1 \to \Omega_1$ is a L^2 isometry, the spectra of $\triangle|_{\mathrm{d}\Omega_0}$ and $\triangle|_{\delta\Omega_2}$ coincide. Hence $\mathrm{spec}\,\triangle_{\Omega_1}$ is $\mathrm{spec}\,\triangle|_{\mathrm{d}\Omega_0}$ with double multiplicity. In fact,

$$\mathrm{spec}\,\triangle|_{\mathrm{d}\Omega_0} = \mathrm{spec}\,\triangle_{\Omega_0} \backslash \{0\}. \tag{4.32}$$

To see this, let $\nu \in \mathrm{spec}\,\triangle_{\Omega_0}$ and Y_0 be the corresponding eigenfunction. Then

$$\triangle \mathrm{d}Y_0 = \mathrm{d}\triangle Y_0 = \mathrm{d}\nu Y_0 = \nu \mathrm{d}Y_0 \tag{4.33}$$

so if $\mathrm{d}Y_0 \neq 0$ (that is, $\nu \neq 0$), then $\nu \in \mathrm{spec}\,\triangle|_{\mathrm{d}\Omega_0}$. Conversely, let $\nu \in \mathrm{spec}\,\triangle|_{\mathrm{d}\Omega_0}$ and $\mathrm{d}Y_0$ be the corresponding eigenform. Then $\nu \neq 0$ (since there is no harmonic one-form on S^2), so

$$
\begin{aligned}
0 = \triangle \mathrm{d}Y_0 - \nu \mathrm{d}Y_0 &= \mathrm{d}(\triangle Y_0 - \nu Y_0) \\
\Rightarrow \quad \triangle Y_0 - \nu Y_0 &= c, \quad \text{constant} \\
\Rightarrow \quad \triangle Y_0' - \nu Y_0' &= 0, \quad \text{where } Y_0' = Y_0 + \tfrac{c}{\nu}
\end{aligned}
\tag{4.34}
$$

and hence $\nu \in \mathrm{spec}\,\triangle_{\Omega_0}$. The spectrum of $\triangle_{\Omega_0}$ is well known.

We conclude that, at $\mu = 1$ (equivalently $\lambda = 0$),

$$
\begin{aligned}
\mathrm{spec}\,\mathscr{J}_\varphi &= \{\ell(\ell+1) - 2 : \ell \in \mathbb{Z}^+\} \\
\mathrm{multiplicity}(\ell(\ell+1) - 2) &= 4\ell + 2.
\end{aligned}
\tag{4.35}
$$

Since we know the eigenvalues (and eigensections) of $\mathscr{J}_\varphi$ at $\lambda = 0$, we can use these as seed data for the numerical shooting method, starting at $\lambda = 0$ and increasing λ in small steps. In this way we can numerically construct curves $\omega_i^2(\lambda)$ showing how the different eigenvalues vary with lump sharpness λ. Figure 1 shows such curves for the lowest 48 eigenvalues. Recall that the eigenvalue 0 has multiplicity 6 (the dimension of the moduli space), and that other eigenvalues always have multiplicity (at least) 2 due to the symmetry under J^N (or, equivalently, due to the block structure of $\mathscr{J}_\varphi$ on I_m).

It is interesting to examine the $\lambda \to \infty$ behaviour of $\omega_i^2(\lambda)$. The pointwise limit of $\varphi : S^2 \to S^2$ as $\lambda \to \infty$ is

$$
\varphi_\infty(p) = \begin{cases} (0,0,1) & p \neq (0,0,-1) \\ (0,0,-1) & p = (0,0,-1) \end{cases}
\tag{4.36}
$$

that is, φ_∞ is constant almost everywhere. A sensible guess for the limiting spectrum would, therefore, be the spectrum of the Jacobi operator at a constant map, which is known to coincide
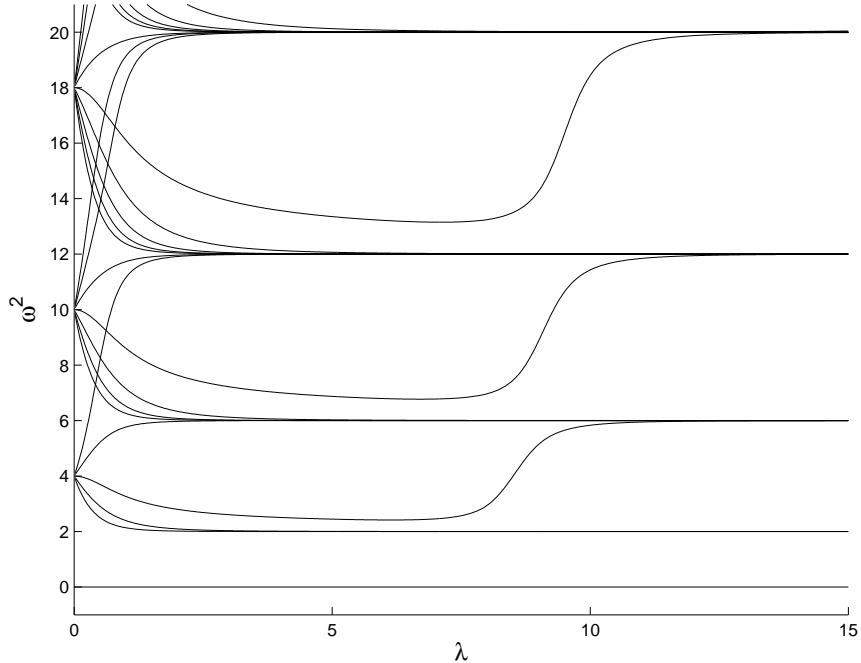
Figure 1: The dependence of the eigenvalues of the Jacobi operator $\mathscr{J}_\varphi$ on the lump sharpness λ. Note that the eigenvalues interpolate between $\ell(\ell+1) - 2$, $\ell \in \mathbb{Z}^+$, at $\lambda = 0$ and $\ell(\ell+1)$, $\ell \in \mathbb{N}$ as $\lambda \to \infty$.

with n copies of the spectrum of the Laplacian on functions, where n is the dimension of the codomain [40, p160]. In this case

$$
\begin{aligned}
\text{spec } \mathscr{J}_{\text{const}} &= \{\ell(\ell+1) : \ell \in \mathbb{N}\} \\
\text{multiplicity}(\ell(\ell+1)) &= 4\ell + 2.
\end{aligned}
\tag{4.37}
$$

The numerics suggest that this guess for the limiting spectrum is very nearly correct. Specifically, the eigenvalues do tend, as $\lambda \to \infty$ to eigenvalues of $\mathscr{J}_{\text{const}}$, and, apart from the eigenvalues 0 and 2, those eigenvalues tending to $\ell(\ell+1)$ have total multiplicity $4\ell + 2$. So the guess is wrong only in that it predicts the multiplicity of the limiting eigenvalue 0 to be 2 rather than 6 (as it must be given the dimension of Rat_1) and the multiplicity of 2 to be 6 rather than 4 (as found numerically).

4.2 The regularized Casimir energy

Having computed spec $\mathscr{J}_\varphi$, we must now try to make sense of the Casimir energy $\mathscr{C}(\lambda)$ in (4.1) which, as it stands, is divergent. It is conventional to reset the zero of potential energy so that the total zero-point energy of the vacuum is 0. For our purposes, φ_∞ is (almost everywhere) the vacuum, so it is convenient to define

$$
\mathscr{C}_k(\lambda) = \frac{1}{2} \sum_{i=1}^{k} (\omega_i(\lambda) - \omega_i(\infty)),
\tag{4.38}
$$

15

where the eigenvalues $\omega_i(\lambda)^2 > 0$ are arranged in such a way that $\omega_i(0)^2$ is nondecreasing.

One option would be to renormalize the spectrum (4.38) numerically, using for example the heat kernel approach. Here, we will employ a different semi-analytical approach. We first discuss the finite sums $\mathscr{C}_k$ for special values of k and then describe how we regularize the diverging sum as $k \to \infty$. We choose $k = 10$, $k = 24$ and $k = 42$, which include the lowest 1, 2 and 3 eigenvalues of $\mathscr{J}_{\mathrm{Id}}$ respectively. Note that, since we have eigenvalue crossings in figure 1, this amounts to the lowest k normal modes at $\lambda = 0$, but not at large λ (where the eigenvalue ordering has changed). If we were to define $\mathscr{C}_k(\lambda)$ as the sum of the frequencies of the lowest k normal modes at each λ, the function $\mathscr{C}_k$ would not be smooth (it would have corners where eigenvalues cross). In effect, we are making a large but finite-dimensional approximation to the quantum field theory, in which the wavefunction is a function on a vector bundle over Rat_1, whose fibre over φ is a union of low-lying eigenspaces of $\mathscr{J}_\varphi$. We are choosing these eigenspaces so that they vary smoothly over Rat_1. The price for this is that they are, towards the boundary of Rat_1, not quite the lowest energy eigenspaces available up to dimension k.
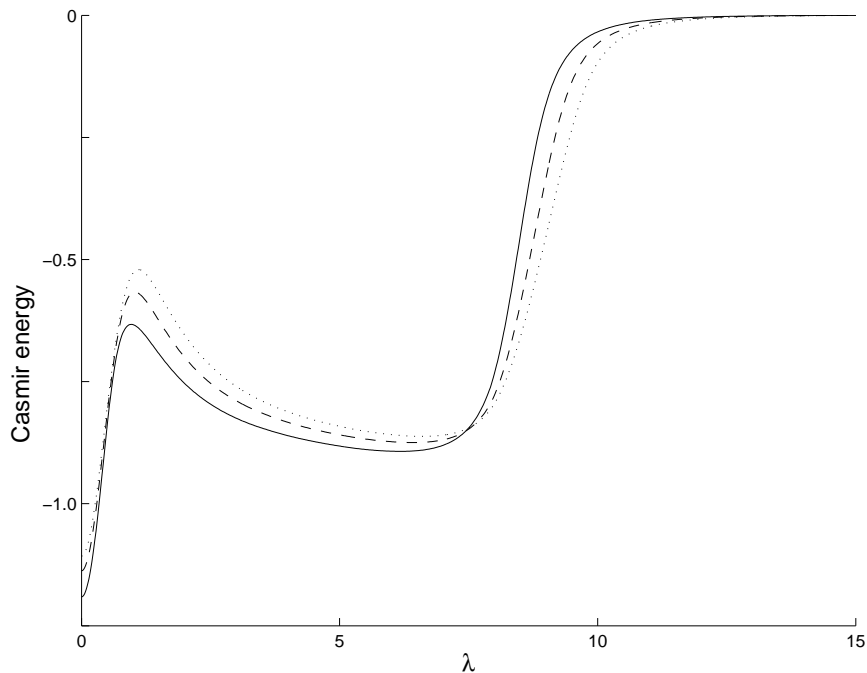

Figure 2: The one-lump Casimir energy as a function of lump sharpness λ for three different cut-offs: solid curve $\mathscr{C}_{10}(\lambda)$, dashed curve $\frac{1}{2}\mathscr{C}_{24}(\lambda)$, dotted curve $\frac{1}{3}\mathscr{C}_{42}(\lambda)$, where $\mathscr{C}_k$ is defined in (4.38). The values $k = 10$, $k = 24$ and $k = 42$ correspond to the lowest 1, 2, and 3 eivenvalues of $\mathcal{J}_{\mathrm{Id}}$, respectively.

Plots of $\mathscr{C}_{10}$, $\mathscr{C}_{24}$ and $\mathscr{C}_{42}$ are presented in figure 2. The curves for $\mathscr{C}_{24}$ and $\mathscr{C}_{42}$ have been rescaled vertically, by a factor of $\frac{1}{2}$ and $\frac{1}{3}$ respectively, to make comparison with $\mathscr{C}_{10}$ easier. Note that these three functions are qualitatively very similar. In fact, the Casimir curves $\mathscr{C}_{10}$, $\mathscr{C}_{24}$ and $\mathscr{C}_{42}$ are approximately self-similar up to a factor which diverges as $k \to \infty$. We have opted to use the self-similarity and regularize the diverging factor (the depth of the well at

$\lambda = 0$). So we define the approximate renormalized Casimir energy $\mathscr{C}(\lambda)$ to be

$$\mathscr{C}(\lambda) = C_* \frac{\mathscr{C}_{10}(\lambda)}{|\mathscr{C}_{10}(0)|} \tag{4.39}$$

where C_* is the renormalized Casimir energy of the $\lambda = 0$ lump. This can be computed exactly using zeta function regularization, because, as we have seen the spectra of the Jacobi operator for the identify map ($\lambda = 0$ lump) and the constant map (the vacuum) are known exactly.

4.3 Zeta function regularization

For $\lambda = 0$, the spectrum of the Jacobi operator is known explicitly, namely $\omega_0^2 = 0$ with multiplicity $\mu_0 = 6$ and $\omega_l^2 = l(l+3)$ with multiplicity $\mu_l = 4l+6$ for $l = 1, 2, \ldots$ This enables us to calculate the Casimir energy using zeta function regularization. The key idea is to write down the corresponding zeta function

$$\zeta(s) = \sum_{l=1}^{\infty} \mu_l \left(\omega_l^2 \right)^{-s}, \tag{4.40}$$

leaving out the zero modes. The zeta function (4.40) is absolutely convergent as long as the real part of s is sufficiently large. In this region, $\zeta(s)$ can be viewed as an analytic function of s. We are interested in the Casimir energy which corresponds to the value $s = -\frac{1}{2}$. In this case, the formal sum in (4.40) is divergent, however, $\zeta(s)$ defined as analytic continuation is well-defined. It is convenient to rewrite $\zeta(s)$ as the following sum:

$$\zeta(s) = \sum_{l=1}^{\infty} 2l(l(l+3))^{-s} + \sum_{l=1}^{\infty} 2(l+3)(l(l+3))^{-s} \tag{4.41}$$

then we can use formula (5.8) in [9, p. 122] to obtain

$$\zeta(-\tfrac{1}{2}) = -2.373.$$

The corresponding calculation for the vacuum, whose spectrum is $\omega_l^2 = l(l+1)$ with multiplicity $\mu_l = 4l+2$, leads to the zeta function

$$\zeta(s) = \sum_{l=1}^{\infty} 2l(l(l+1))^{-s} + \sum_{l=1}^{\infty} 2(l+1)(l(l+1))^{-s} \tag{4.42}$$

and yields

$$\zeta_{\mathrm{vac}}(-\tfrac{1}{2}) = -0.530.$$

See also equation (5.34) in [9, p. 126]. Hence, the Casimir energy of the $\lambda = 0$ lump on the unit two-sphere can be evaluated using

$$\frac{1}{2} \left(\zeta(-\tfrac{1}{2}) - \zeta_{\mathrm{vac}}(-\tfrac{1}{2}) \right) = -0.921.$$

Hence
$$C_* = |\mathscr{C}(0)| = 0.921.$$
This is the energy scale we used to set the renormalized energy scale for our numerically generated Casimir energy function $\mathscr{C}(\lambda)$ in (4.39).

Our approximation to the Casimir energy $\mathscr{C}(\lambda)$ is now given by the rescaled and shifted curve $\mathscr{C}_{10}(\lambda)$ in figure 2. It is non-singular and appears to be smooth. It is worth summarizing the approximations involved. Our calculation relies on a conjectured self-similarity of the curves in figure 2. We also assume that we can neglect the effects of crossing modes. In particular, we assume that the zeta-function regularization can be performed pointwise when we regularize the Casimir energy at $\lambda = 0$ and $\lambda = \infty$. Furthermore, we assume that the $\mathscr{C}(\lambda) \to 0$ as $\lambda \to 0$ because the lumps converge almost everywhere to the vacuum in that limit.

The obvious alternative to our approach, namely a numerical evaluation using heat kernel or zeta function regularization as in [29, 27], is beyond the scope of this paper.

5   The energy spectra

In the following, we describe how to calculate the spectrum of the Laplacian (3.2). In order to make use of the physics literature on this topic we rewrite the Laplacian using angular momentum operators. Note that the operators $\mathbf{J} = -i\boldsymbol{\theta}$, $\mathbf{L} = -i\boldsymbol{\lambda} \times \boldsymbol{\partial}$, $\mathbf{T} = \mathbf{J} + \mathbf{L}$ and $\mathbf{K} = -i\boldsymbol{\xi}$ all satisfy the canonical commutation relations for angular momenta, namely,

$$[X_1, X_2] = iX_3, \qquad \mathbf{X} = \mathbf{J}, \mathbf{K}, \mathbf{L}, \mathbf{T}$$

and cyclic permutations. Recall that $i\mathbf{K}$ generates the left $SO(3)$ action, on the target S^2, and $i\mathbf{T}$ generates the right $SO(3)$ action, on the physical S^2, so we refer to these operators as isospin and spin respectively. Making use of these operators, one sees that the Laplacian (3.2) is

$$\begin{aligned}
\triangle\psi &= -\frac{1}{\Lambda\lambda^2 A^2 B}\frac{\partial}{\partial\lambda}\left(\frac{\lambda^2\Lambda^3 A^2}{4}\frac{\partial\psi}{\partial\lambda}\right) + \frac{1}{\lambda^2\Lambda^2 A}\mathbf{L}^2\psi \\
&\quad + \frac{2}{\Lambda^2 A}\left\{\mathbf{J}^2\psi + \mathbf{T}^2\psi - \frac{2}{\lambda^2}\left[1 - \frac{\Lambda^2 A}{4B}\right](\boldsymbol{\lambda}\cdot\mathbf{T})^2\psi\right\}.
\end{aligned} \tag{5.1}$$

Here, we replaced the $\mathbf{L}\cdot\mathbf{J}$ term using the convenient operator identity

$$2\mathbf{L}\cdot\mathbf{J} = \mathbf{T}^2 - \mathbf{L}^2 - \mathbf{J}^2. \tag{5.2}$$

We have already shown that $\triangle$ commutes with $\mathbf{T}$ and $\mathbf{K}$, as it must, by $SO(3) \times SO(3)$ invariance. In fact, the operators $\triangle, |\mathbf{T}|^2, T_3, |\mathbf{K}|^2, K_3, P$, where $P : \boldsymbol{\lambda} \mapsto -\boldsymbol{\lambda}$ is the parity operator, all mutually commute, so we can seek simultaneous eigenstates of these six operators.

5.1 Spin-isospin interchange symmetry

Let $t(t+1)$ and $k(k+1)$ be the eigenvalues of $|\mathbf{T}|^2$ and $|\mathbf{K}|^2$. It is a somewhat surprising fact that the spectrum of $\triangle$ is invariant under interchange of t and k. Even more surprising is that this remains true even if we give the physical and target spheres different radii. The key to seeing this is the following isometry of any $SO(3) \times SO(3)$ invariant kähler metric on Rat_1.

Proposition 6 *Identify $\mathsf{Rat}_1 \cong SO(3) \times \mathbb{R}^3$ with $TSO(3)$ via $(R, \boldsymbol{\lambda}) \equiv (\boldsymbol{\lambda} \cdot \boldsymbol{\theta})(R) \in T_R SO(3)$. The mapping $f : SO(3) \to SO(3)$, $f(R) = R^{-1}$ induces a mapping $df : TSO(3) \to TSO(3)$. Then df is an isometry of any $SO(3) \times SO(3)$ invariant kähler metric on $TSO(3)$.*

Proof: The identification $\mathsf{Rat}_1 \equiv TSO(3)$ amounts to thinking of $\boldsymbol{\lambda}$ as a vector in the Lie algebra $\mathfrak{so}(3)$ (skew 3×3 real matrices) and identifying $T_R SO(3)$ with $\mathfrak{so}(3) = T_e SO(3)$ by left translation. Hence, the map in question is

$$df : (R, \boldsymbol{\lambda}) \mapsto (R^{-1}, -Ad_R \boldsymbol{\lambda}).$$

Let $q(t) = (R(t), \boldsymbol{\lambda}(t))$ be a curve in Rat_1 with $\dot{q}(0) = (R(0)\boldsymbol{\Omega}, \boldsymbol{v})$, $\boldsymbol{\Omega}, \boldsymbol{v} \in \mathfrak{so}(3)$. Then, with respect to the $SO(3) \times SO(3)$ invariant kähler metric determined by the functions $A_i(\lambda)$, as in Proposition 1,

$$\|\dot{q}(0)\|^2 = A_1 |\boldsymbol{v}|^2 + A_2 (\boldsymbol{\lambda} \cdot \boldsymbol{v})^2 + A_3 |\boldsymbol{\Omega}|^2 + A_4 (\boldsymbol{\lambda} \cdot \boldsymbol{\Omega})^2 + A_1 \boldsymbol{v} \cdot (\boldsymbol{\lambda} \times \boldsymbol{\Omega}).$$

The image of this curve under df is $\widetilde{q}(t) = (R^{-1}(t), -R(t)\boldsymbol{\lambda}(t)R^{-1}(t))$, which has $\dot{\widetilde{q}}(0) = (R^{-1}(0)\widetilde{\boldsymbol{\Omega}}, \widetilde{\boldsymbol{v}})$, where

$$(\widetilde{\boldsymbol{\Omega}}, \widetilde{\boldsymbol{v}}) = -(Ad_R \boldsymbol{\Omega}, Ad_R(\boldsymbol{v} - [\boldsymbol{\lambda}, \boldsymbol{\Omega}]_{\mathfrak{so}(3)})).$$

Recalling that the Lie bracket on $\mathfrak{so}(3)$ coincides with minus the vector product on $\mathbb{R}^3$ under the natural identification $\mathfrak{so}(3) \equiv \mathbb{R}^3$, and the adjoint action of $SO(3)$ on $\mathfrak{so}(3)$ coincides with the fundamental action on $\mathbb{R}^3$, we find that

$$\begin{aligned}
\|\dot{\widetilde{q}}(0)\|^2 &= A_1 |\boldsymbol{v} + \boldsymbol{\lambda} \times \boldsymbol{\Omega}|^2 + A_2 (\boldsymbol{\lambda} \cdot \boldsymbol{v})^2 + A_3 |\boldsymbol{\Omega}|^2 + A_4 (\boldsymbol{\lambda} \cdot \boldsymbol{\Omega})^2 - A_1 (\boldsymbol{v} + \boldsymbol{\lambda} \times \boldsymbol{\Omega}) \cdot (\boldsymbol{\lambda} \times \boldsymbol{\Omega}). \\
&= \|\dot{q}(0)\|^2.
\end{aligned}$$

Hence df is an isometry, as claimed. $\qquad\square$

Proposition 7 *Given $E \in \mathbb{R}$ and $k, t \in \mathbb{N}$, denote by $X_{E,k,t}$ the simultaneous eigenspace of*

$$H = \tfrac{1}{2}\triangle + V, \qquad |\mathbf{K}|^2, \qquad |\mathbf{T}|^2$$

with eigenvalues E, $k(k+1)$ and $t(t+1)$, where $V : \mathsf{Rat}_1 \to \mathbb{R}$ is any $SO(3) \times SO(3)$ invariant potential. Then $X_{E,k,t}$ and $X_{E,t,k}$ have equal dimension.

Proof: Under the identification $\mathsf{Rat}_1 \equiv TSO(3)$, the left and right actions of $SO(3)$ on Rat_1 coincide with the natural left and right actions of $SO(3)$ on $TSO(3)$. Denote by df^* the induced map on $L^2(TSO(3), \mathbb{C})$, $df^*\psi = \psi \circ df$. Then, since df is an isometry and preserves the length of $\boldsymbol{\lambda}$, $Hdf^* = df^*H$. Furthermore, df interchanges the left and right $SO(3)$ actions on $TSO(3)$,

so $\mathbf{K}df^* = -df^*\mathbf{T}$ and $\mathbf{T}df^* = -df^*\mathbf{K}$. Hence, $df^* : X_{E,k,t} \to X_{E,t,k}$ and $df^* : X_{E,t,k} \to X_{E,k,t}$ for all E, k, t. Now $df^2 = \mathrm{Id}$, so $(df^*)^2 = \mathrm{Id}$, and hence df^* is invertible, so the eigenspaces $X_{E,k,t}$ and $X_{E,t,k}$ are isomorphic. $\qquad\square$

Note that this k, t interchange symmetry holds for *any* invariant kähler metric on Rat_1, so is not special to the case where the domain and target two-spheres have equal radius. Also note that it relies heavily on the kähler property of the metric, and does not follow from $SO(3) \times SO(3)$ invariance alone (or, indeed, just invariance and hermiticity). This is a "hidden" symmetry which one cannot see directly from the field theory. It is an interesting question whether a direct physical argument can be given to explain this symmetry. A construction involving a supersymmetric extension of the model would be a natural candidate.

5.2   Reduction to a Sturm-Liouville problem

The wavefunction is a function $\psi : SO(3) \times \mathbb{R}^3 \to \mathbb{C}$. According to the Peter-Weyl theorem [16], the matrix elements of all irreducible unitary representations of the group $SO(3)$ form an orthonormal basis for $L^2(SO(3), \mathbb{C})$. Recall that such representations are labelled by $k \in \{0, 1, 2, \ldots\}$, and that the matrix elements of the k representation are functions $\pi^{(k)}_{j_3,k_3} : SO(3) \to \mathbb{C}$ where $-k \le j_3, k_3 \le k$. We have chosen the symbol k to label the representations because

$$|\mathbf{K}|^2 \pi^{(k)}_{j_3,k_3} = |\mathbf{J}|^2 \pi^{(k)}_{j_3,k_3} = k(k+1)\pi^{(k)}_{j_3,k_3}. \tag{5.3}$$

Further, we may choose the basis for $\mathbb{C}^{2k+1}$ so that

$$K_3 \pi^{(k)}_{j_3,k_3} = k_3 \pi^{(k)}_{j_3,k_3}, \qquad J_3 \pi^{(k)}_{j_3,k_3} = j_3 \pi^{(k)}_{j_3,k_3}, \tag{5.4}$$

which is why we have labelled the matrix elements with j_3, k_3. For the $\mathbb{R}^3$ dependence of ψ we use spherical polar coordinates and expand the angular dependence in spherical harmonics. Hence we may express the wavefunction as follows,

$$\psi = \sum_{k=0}^{\infty} \sum_{l=0}^{\infty} \sum_{j_3=-k}^{k} \sum_{k_3=-k}^{k} \sum_{l_3=-l}^{l} a^{k,l}_{j_3,k_3,l_3}(\lambda)\, |k, l, j_3, k_3, l_3\rangle, \tag{5.5}$$

where

$$|k, l, j_3, k_3, l_3\rangle = \pi^{(k)}_{j_3,k_3} Y_{l,l_3}, \tag{5.6}$$

and $Y_{l,l_3} : S^2 \to \mathbb{C}$ denote spherical harmonics.

Recall that $H, |\mathbf{K}|^2, K_3, |\mathbf{T}|^2, T_3$ are mutually commuting, so we may solve the eigenvalue problem for H on each simultaneous eigenspace of $|\mathbf{K}|^2, K_3, |\mathbf{T}|^2, T_3$ separately. Clearly, H is independent of k_3 and t_3 so we may, and henceforth will, without loss of generality, set $k_3 = t_3 = 0$, remembering to multiply all degeneracies by $(2k+1)(2t+1)$ to account for the other values of (k_3, t_3). Furthermore, by Proposition 7 we may, without loss of generality, assume that $k \le t$, doubling the multiplicity if $k < t$. Recall that $\mathbf{T} = \mathbf{J} + \mathbf{L}$ and that $\mathbf{J}$ and $\mathbf{L}$ satisfy the angular momentum algebra. Hence a basis $\{|k, t, l\rangle \, : \, |k - t| \le l \le k + t\}$ for

the $(k, 0, t, 0)$ eigenspace can be constructed, using Clebsch-Gordon coefficients, on which the operators $|\mathbf{J}|^2 = |\mathbf{K}|^2$, $|\mathbf{T}|^2$, $|\mathbf{L}|^2$ act naturally

$$|\mathbf{J}|^2 |k, t, l\rangle = k(k+1) |k, t, l\rangle \tag{5.7}$$

$$|\mathbf{T}|^2 |k, t, l\rangle = t(t+1) |k, t, l\rangle \tag{5.8}$$

$$|\mathbf{L}|^2 |k, t, l\rangle = l(l+1) |k, t, l\rangle, \tag{5.9}$$

see Appendix B for details.

By expanding the wavefunction as $\psi = \sum_{l=|k-t|}^{k+t} a_l(\lambda) |k, t, l\rangle$, we may express the Hamiltonian $H = \frac{1}{2}\triangle + V$ as a $m \times m$ matrix of differential operators acting on the vector function $a : [0, \infty) \to \mathbb{C}^m$, where $m = 2\min(k, t) + 1$. Its structure is

$$Ha = -p_1(\lambda)\frac{d}{d\lambda}\left(p_2(\lambda)\frac{da}{d\lambda}\right) + p_3(\lambda)M_1 a + p_4(\lambda)(k(k+1) + t(t+1))a + p_5(\lambda)M_2 a + V(\lambda)a \tag{5.10}$$

where $p_i(\lambda)$ are rather complicated but explicitly known functions of λ (see Proposition 4) and M_1, M_2 are $m \times m$ matrices corresponding to $\mathbf{L}^2$ and $(\boldsymbol{\lambda} \cdot \mathbf{T})^2$ respectively. By our choice of basis, M_1 is diagonal and has entries $l(l+1)$ with l running from $|k-t|$ (top left) to $k+t$ (bottom right). The matrix M_2 corresponding to operator $(\boldsymbol{\lambda} \cdot \mathbf{T})^2$ is the only non-diagonal term in the Hamiltonian and is discussed in more detail in appendix B. It mixes states of different l, which differ by 2. This leads to a natural chess board structure. Hence, by a reordering of the basis vectors, the operator can be written in block diagonal form with one block corresponding to the states with even l and the other block to odd l. These blocks correspond to the decompostion of the $(k, 0, t, 0)$ eigenspace into $P = +1$ (even l) and $P = -1$ (odd l) parity eigenspaces noting that $PY_{l,m} = (-1)^l Y_{l,m}$. In summary, for fixed (k, t), the eigenvalue problem for any Hamiltonian of the form $H = \frac{1}{2}\triangle + V(\lambda)$ reduces to a matrix-valued Sturm-Liouville problem on $[0, \infty)$ of dimension $m = 2\min(k, t) + 1$.

5.3 Boundary conditions

We can now address the eigenvalue equations

$$H_i a = Ea, \tag{5.11}$$

where E is the energy eigenvalue, and the Hamiltonians H_0, H_1 and H_2 are given by (1.3). As just explained, the spectral problem reduces to a sequence of matrix-valued Sturm-Liouville problems indexed by $t \in \{0, 1, 2, \ldots\}$ and $k \in \{0, 1, \ldots, t\}$, where each subproblem has dimension $2\min(k, t) + 1$. In order to calculate the spectrum of the Hamiltonians H_0, H_1 and H_2 we have to derive not only the relevant differential equations but also the appropriate boundary conditions. For many important examples in mathematical physics, the boundary conditions are determined solely by the requirement that the wavefunction be L^2 finite. However, in our case, L^2 finiteness is not always sufficient, and we have to apply the theory of singular Sturm-Liouville equations, following [30].

The asymptotic behaviour of the L^2 metric on Rat_1 can be obtained by direct calculation:

$$\begin{array}{llll} A(\lambda) \sim \frac{32\pi}{3} & \text{as } \lambda \to 0, & A(\lambda) \sim \frac{8\pi}{\lambda^2} & \text{as } \lambda \to \infty, \\ B(\lambda) \sim \frac{8\pi}{3} & \text{as } \lambda \to 0, & B(\lambda) \sim \frac{4\pi\log\lambda}{\lambda^4} & \text{as } \lambda \to \infty. \end{array} \tag{5.12}$$

Using the above limits, we obtain the leading order equation for $(H_0 - E)f = 0$ as $\lambda \to \infty$,

$$\frac{\partial^2 f}{\partial \lambda^2} + \frac{1}{\lambda}\frac{\partial f}{\partial \lambda} - \frac{4}{\lambda^2}\left(\hat{\boldsymbol{\lambda}} \cdot \mathbf{T}\right)^2 f = 0, \quad \text{with} \quad \hat{\boldsymbol{\lambda}} = \frac{\boldsymbol{\lambda}}{\lambda}, \tag{5.13}$$

and the leading order equation for $(H_0 - E)f = 0$ as $\lambda \to 0$,

$$\frac{\partial^2 f}{\partial \lambda^2} + \frac{2}{\lambda}\frac{\partial f}{\partial \lambda} - \frac{l(l+1)}{\lambda^2}f = 0. \tag{5.14}$$

For $\lambda \to 0$ equation (5.11) for H_0 has a regular singular point. The asymptotic form of the solutions can be derived from (5.14) and is given by[1]

$$f(\lambda) = c_1 \lambda^l + c_2 \lambda^{-l-1}. \tag{5.15}$$

Note that the leading order asymptotic behaviour is independent of the energy eigenvalue E. We are interested in solutions that are L^2 finite which leads to the condition

$$\int f^2 \text{vol} < \infty. \tag{5.16}$$

Using polar coordinates for (3.4) we obtain the two asymptotic behaviours,

$$f^2\text{vol} \sim \tilde{c}_1 \lambda^{2l+2} \quad \text{and} \quad f^2\text{vol} \sim \tilde{c}_2 \lambda^{-2l},$$

for suitable constants $\tilde{c}_1$ and $\tilde{c}_2$. Hence $l > 0$ corresponds to the limit-point case, since only the first solution is L^2 finite, see e.g. [30] for further details. However, for $l = 0$ the situation is slightly more subtle. Both asymptotic solutions are L^2 finite. This is known as the limit-circle case.[2] The Hamiltonians H_1, H_2 lead to the same asymptotic behaviour since the curvature and Casimir energy are finite as $\lambda \to 0$.

For $\lambda \to \infty$ it is convenient to analyse the boundary conditions in a different basis so that the operator $(\hat{\boldsymbol{\lambda}} \cdot \mathbf{T})$ is diagonal,

$$\left(\hat{\boldsymbol{\lambda}} \cdot \mathbf{T}\right)^2 f = p^2 f,$$

where the integer k satisfies $-\min(k,t) \leq p \leq \min(k,t)$, see appendix B. Then the asymptotic solution follows from (5.13) and is given by

$$f(\lambda) = c_1 \lambda^{-2p} + c_2 \lambda^{2p}, \tag{5.17}$$

for $p \neq 0$ and

$$f(\lambda) = c_1 + c_2 \log(\lambda), \tag{5.18}$$

for $p = 0$. Again the leading order behaviour is independent of the energy eigenvalue E.

Both H_1 and H_2 contain the scalar curvature function $\kappa(\lambda)$ which is known to diverge to infinity as $\lambda \to \infty$. In fact, using the formula obtained in [37], and accounting for the change

---

[1]Higher order terms in the expansions for $\lambda \to 0$ and $\lambda \to \infty$ have been calculated in [24] for H_0 with $k = 0$.

[2]The same subtlety occurs when solving the Schrödinger equation for the hydrogen atom in spherical polar coordinates.

in normalizations (recall we are giving the domain and target spheres unit radius), we find the asymptotic formula

$$\kappa(\lambda) \sim \frac{1}{16\pi} \frac{\lambda^4}{\log \lambda} \qquad \text{as } \lambda \to \infty. \tag{5.19}$$

This adds a term to (5.13), namely,

$$\frac{\partial^2 f}{\partial \lambda^2} + \frac{1}{\lambda} \frac{\partial f}{\partial \lambda} - \frac{1}{\lambda^2} \left(4 \left(\hat{\boldsymbol{\lambda}} \cdot \mathbf{T} \right)^2 + \frac{1}{2 \log(\lambda)^2} \right) f = 0. \tag{5.20}$$

For $p \neq 0$ we can solve (5.20) in terms of modified Bessel functions

$$f(\lambda) = c_1 \sqrt{\log \lambda} K_{\sqrt{3}/2} \left(2p \log(\lambda) \right) + c_2 \sqrt{\log \lambda} I_{\sqrt{3}/2} \left(2p \log(\lambda) \right). \tag{5.21}$$

With the help of asymptotic expansions, see e.g. [1], it can be shown that the leading order is identical to (5.17). For $p = 0$ we obtain

$$f(\lambda) = c_1 \log(\lambda)^{\frac{1}{2} - \frac{1}{2}\sqrt{3}} + c_2 \log(\lambda)^{\frac{1}{2} + \frac{1}{2}\sqrt{3}}. \tag{5.22}$$

Since the Casimir energy is bounded, the asymptotic behaviour of H_2 as $\lambda \to \infty$ is the same as H_1.

As $\lambda \to \infty$ the L^2 finite condition (5.16) again leads to two asymptotic behaviours,

$$f^2 \text{vol} \sim \tilde{c}_1 \log(\lambda)\lambda^{-2p-5} \quad \text{and} \quad f^2 \text{vol} \sim \tilde{c}_2 \log(\lambda)\lambda^{2p-5},$$

for suitable constants $\tilde{c}_1$ and $\tilde{c}_2$ in the case $p > 0$. For $p = 0$, the curvature term has an influence on the asymptotic behaviour. For H_0, we obtain

$$f^2 \text{vol} \sim \tilde{c}_1 \log(\lambda)\lambda^{-5} \quad \text{and} \quad f^2 \text{vol} \sim \tilde{c}_2 \log(\lambda)^2 \lambda^{-5},$$

whereas for H_1 and H_2 the asymptotic behaviour is

$$f^2 \text{vol} \sim \tilde{c}_1 \log(\lambda)^{\frac{3}{2} - \frac{\sqrt{3}}{2}} \lambda^{-5} \quad \text{and} \quad f^2 \text{vol} \sim \tilde{c}_2 \log(\lambda)^{\frac{3}{2} + \frac{\sqrt{3}}{2}} \lambda^{-5}.$$

Hence for $p < 2$ both solutions lead to L^2 finite solutions, resulting in a limit-circle case.

In summary, for all values of k and t the boundary conditions are either of limit-circle or of limit-point type. Furthermore, both end points are non-oscillatory and independent of the energy eigenvalue E. This allows us to apply theorem 7.5 in [30] which ensures that the spectrum is purely discrete, bounded below and unbounded above.

If limit-circle endpoints are present, a Sturm-Liouville problem is not self-adjoint unless boundary conditions are imposed. For a non-oscillatory endpoint a there is always one solution which is "small", known as the subdominant solution. More precisely, the subdominant solution $u(\lambda)$, unique up to a scalar factor, satisfies

$$\lim_{\lambda \to a} \frac{u(\lambda)}{v(\lambda)} = 0, \tag{5.23}$$

where $v(\lambda)$ is any linearly independent solution, see theorem 7.15(i) in [30]. In our case, the subdominant solution is the non-singular solution, e.g. $c_1 \lambda^l$ as $\lambda \to 0$. A natural boundary condition is defined by the subdominance condition, i.e. always taking the non-singular solution. Theorem 7.21 in [30] then guarantees that the subdominance condition defines a valid self-adjoint problem known as the Friedrichs extension.

5.4 Numerical results

In the following, we briefly sketch our numerical scheme for H_0 with k and t fixed. The equations for H_1 and H_2 require minor, but straightforward modifications. We are using a multi-component shooting method which solves a collection of initial value problems (for the eigenvalue equation at fixed E) numerically with a standard adaptive Runge-Kutta method. The first initial value problem has initial values at $\lambda_0 \approx 0$ and the solution $a(\lambda)$ of the differential equation (5.11) is evaluated at a matching point $\lambda_m \gg \lambda_0$. Allowing the initial data to span the $m = 2 \min(k, t) + 1$ dimensional space specified by the boundary condition at 0, this produces a $2m \times m$ matrix ϕ whose columns consist of $a(\lambda_m)$ above $a'(\lambda_m)$. The second initial value problem has initial values at $\lambda_\infty \gg \lambda_m$ and is again evaluated at λ_m, resulting, as the initial data span the boundary condition, in a $2m \times m$ matrix η constructed similarly. By construction, a general solution satisfying the boundary condition at 0 lies, at λ_m, in the column span of ϕ, while a general solution satisfying the boundary condition at ∞ lies, at λ_m in the column span of η. Hence, E is an eigenvalue if these spans have nontrivial intersection, that is, if

$$d(E) = \det(\phi \eta) = 0. \tag{5.24}$$

Having constructed $d(E)$ numerically, we find its roots using a bisection method. Typical values of our constants are $\lambda_0 = 0.001$, $\lambda_m = 3$ and $\lambda_\infty = 30$.

Table 1 shows the lowest energy levels for $H_0 = \frac{1}{2}\triangle$ which corresponds to the Laplacian for the L^2 metric, for $H_1 = \frac{1}{2}\triangle + \frac{1}{4}\kappa$ which also includes the curvature corrections, and for $H_2 = \frac{1}{2}\triangle + \frac{1}{4}\kappa + \mathscr{C}$ which includes curvature corrections and Casimir energy. Energy levels are rounded to two decimal places. The energy levels are ordered according to their respective energy, and are labelled by isospin quantum number k, total angular momentum quantum number t and parity P. Curly brackets indicate that the states (k, t) and (t, k) have the same energy. States with the same quantum numbers but different energies form sequences of radially excited states. We have chosen to display levels with an energy not greater than the second excited $(k = 0, t = 0)$ state, which are 19 energy levels in total. The columns "degeneracy" give the number of different states with the same energy. For $k = t$, the degeneracy is given by $(2k + 1)^2$, whereas for $k \neq t$ it is $2(2k + 1)(2t + 1)$, where the extra factor of 2 arises from the $(k, t) \to (t, k)$ symmetry of the spectrum.

The spectra of H_0 and H_1 are remarkably similar. The order of the energy levels remains the same apart from two exceptions which are marked with a $*$ in table 1 and which will be discussed in more detail later. The Casimir energy leads to significant changes, nevertheless the spectrum still shares some similarities. The ground state of H_0 has energy $E_0^{(0)} = 0.00$. The curvature term increases the energy of the ground state of H_1 to $E_0^{(1)} = 0.22$, whereas the renormalised Casimir energy leads to a decrease in the ground state of H_2 to $E_0^{(2)} = -0.41$.

In order to compare the energies of the excited states, we shift the spectrum of the ground states of H_1 and H_2 to 0.00 and then calculate the relative difference of the corresponding energy levels. Hence, the relative difference in energy between the nth excited state $E_n^{(0)}$ of H_0 and the nth excited state $E_n^{(1)}$ of H_1 is given by

$$\frac{E_n^{(0)} - \left(E_n^{(1)} - E_0^{(1)}\right)}{E_n^{(0)}}. \tag{5.25}$$

$H_0 = \frac{1}{2}\triangle$			$H_1 = \frac{1}{2}\triangle + \frac{1}{4}\kappa$			$H_2 = \frac{1}{2}\triangle + \frac{1}{4}\kappa + \mathscr{C}$		
energy	degeneracy	$\{k,t\}^P$	energy	degeneracy	$\{k,t\}^P$	energy	degeneracy	$\{k,t\}^P$
0.00	1	$\{0,0\}^+$	0.22	1	$\{0,0\}^+$	-0.41	1	$\{0,0\}^+$
0.13	6	$\{0,1\}^-$	0.38	6	$\{0,1\}^-$	-0.26*	9	$\{1,1\}^+$
0.18	9	$\{1,1\}^+$	0.40	9	$\{1,1\}^+$	-0.19*	6	$\{0,1\}^-$
0.29	1	$\{0,0\}^+$	0.53	1	$\{0,0\}^+$	-0.12	1	$\{0,0\}^+$
0.34	9	$\{1,1\}^+$	0.58	9	$\{1,1\}^+$	-0.01*	9	$\{1,1\}^-$
0.35	10	$\{0,2\}^+$	0.59*	9	$\{1,1\}^-$	0.00*	9	$\{1,1\}^+$
0.38	9	$\{1,1\}^-$	0.61*	10	$\{0,2\}^+$	0.01*	25	$\{2,2\}^+$
0.40	30	$\{1,2\}^-$	0.63	30	$\{1,2\}^-$	0.06	30	$\{1,2\}^-$
0.49	25	$\{2,2\}^+$	0.70	25	$\{2,2\}^+$	0.06*	10	$\{0,2\}^+$
0.54	6	$\{0,1\}^-$	0.80	6	$\{0,1\}^-$	0.15	6	$\{0,1\}^-$
0.62	9	$\{1,1\}^+$	0.83	9	$\{1,1\}^+$	0.22	9	$\{1,1\}^+$
0.63	30	$\{1,2\}^-$	0.87	30	$\{1,2\}^-$	0.29	30	$\{1,2\}^-$
0.64	14	$\{0,3\}^-$	0.88*	30	$\{1,2\}^+$	0.32*	30	$\{1,2\}^+$
0.67	30	$\{1,2\}^+$	0.91*	14	$\{0,3\}^-$	0.33*	25	$\{2,2\}^-$
0.68	25	$\{2,2\}^+$	0.93	25	$\{2,2\}^+$	0.34	25	$\{2,2\}^+$
0.69	42	$\{1,3\}^+$	0.95	42	$\{1,3\}^+$	0.37*	14	$\{0,3\}^-$
0.76	25	$\{2,2\}^-$	0.96	25	$\{2,2\}^-$	0.40*	42	$\{1,3\}^+$
0.79	70	$\{2,3\}^-$	1.01	70	$\{2,3\}^-$	0.41*	1	$\{0,0\}^+$
0.81	1	$\{0,0\}^+$	1.07	1	$\{0,0\}^+$	0.41*	49	$\{3,3\}^+$

Table 1: This table shows the lowest energy eigenvalues of H_0, H_1 and H_2. Each energy eigenvalue is labelled with its degeneracy and its quantum numbers k and t and parity P. Energy eigenvalues marked with a $*$ occur in a different order than their counterpart in the H_0 spectrum.

The relative difference of the $\{0,1\}^-$ states of H_0 and H_1 is 15%, and 7.7% for the first excited $\{0,0\}^+$ state. All the remaining states have a relative difference of less than 7%.

As mentioned earlier, some energy levels change order. Therefore, it is useful to calculate the relative error of states with the same quantum numbers $\{j,t\}^P$. The first transposition occurs for the first $\{0,2\}^+$ state and the first $\{1,1\}^-$ state. The relative difference between the energy of the $\{0,2\}^+$ state between H_0 and H_1 is 10.4%. The second transposition occurs for the first $\{0,3\}^-$ and the first even $\{1,2\}^+$ state, and the $\{0,3\}^-$ state has a relative differences of 8.0%. This leads to the observation that the difference between positive and negative parity states with the same $\{k,t\}$ is reduced for H_1 compared to H_0. Furthermore, H_1 seem to favour states with $k \approx t$.

As can be seen in table 1 the spectrum of H_2 is shows many transpositions compared to the spectra of H_0 and H_1. However, these transpositions occur for states which are close in energy, and the relative positions of the $\{0,0\}^+$ state and the $\{0,0\}^+$ excited states remain almost unchanged. Calculating the relative differences as in formula (5.25) shows that all

relative differences are less than 24%.

5.5   Changing the radii

It is interesting to consider how our results change if the radii R_1, R_2 of the domain and target spheres are altered. We adopt the convention that a tilde signifies the case of general R_1, R_2 while undecorated variables refer to the case $R_1 = R_2 = 1$. It is immediate from (2.4) that the L^2 metric on Rat_n scales as $\widetilde{\gamma} = R_1^2 R_2^2 \gamma$, and hence, from (3.2), we see that the Laplacian scales as $\widetilde{\triangle} = (R_1 R_2)^{-2} \triangle$. Now scalar curvature scales in the same way as the Laplacian (as can easily be seen, in this case, from the formula for κ in [37], for example). Hence, the Hamiltonians H_0 and H_1, scale homogeneously, $\widetilde{H}_i = (R_1 R_2)^{-2} H_i$, and so their spectra can be obtained from table 1 by a simple rescaling. Now the energies shown in this table are quantum *corrections* to the classical energy, which, by the Lichnerowicz bound is $4\pi R_2^2$. Hence, for H_0, H_1, the total energy of the kth energy level is

$$\widetilde{E}_k^{\text{total}} = 4\pi R_2^2 + \frac{E_k}{R_1^2 R_2^2} \tag{5.26}$$

where E_k is the eigenvalue of H_i. It is interesting to note that the quantum correction becomes (naively) dominant in the case of small target space (R_2 small).

The behaviour of H_2 is more subtle because the Casmir energy scales differently from the other terms. To see this, we determine how the Jacobi operator for a harmonic map $\phi : M \to N$ scales under homotheties of M and N.

Proposition 8 Let $\varphi : (M^m, g) \to (N^n, h)$ be harmonic with Jacobi operator $\mathscr{J}$. If $\widetilde{g} = R_1^2 g$, $\widetilde{h} = R_2^2 h$, where $R_1, R_2 > 0$ are constants, then the Jacobi operator of φ as a harmonic map $(M, \widetilde{g}) \to (N, \widetilde{h})$ is

$$\widetilde{\mathscr{J}} = R_1^{-2}\, \mathscr{J}.$$

Proof: Let $\varphi_{s,t} : M \to N$ be a smooth two-parameter variation of $\varphi = \varphi_{0,0}$, with $\partial_s \varphi_{s,t}|_{s=t=0} = X$, $\partial_t \varphi_{s,t}|_{s=t=0} = Y \in \Gamma(\varphi^{-1}TN)$. We have, in obvious notation,

$$
\begin{aligned}
\widetilde{E}(\varphi_{s,t}) &= R_1^{m-2} R_2^2 E(\varphi_{s,t}) \\
\Rightarrow \quad \widetilde{\mathsf{Hess}}(X, Y) &= \left. \frac{\partial^2}{\partial s\, \partial t} \widetilde{E}(\varphi_{s,t}) \right|_{s=t=0} = R_1^{m-2} R_2^2\, \mathsf{Hess}(X, Y) \\
&= R_1^{m-2} R_2^2 \int_M h(X, \mathscr{J}Y)\mathrm{vol} = \int_M \widetilde{h}(X, R_1^{-2}\, \mathscr{J}Y)\widetilde{\mathrm{vol}}.
\end{aligned}
$$

$\square$

Since $\mathscr{C}$ is (formally) a sum of *square roots* of eigenvalues of $\mathscr{J}$, we see that it scales as $\widetilde{\mathscr{C}} = R_1^{-1}\mathscr{C}$. Hence, the scaling behaviour of H_2 is inhomogeneous, and, except in the special case that $R_1 R_2^{-2} = 1$, the spectrum of $\widetilde{H}_2$ cannot be deduced directly from the spectrum of H_2. Since $\mathscr{C}$ is independent of the radius R_2 whereas the spectra of H_0 and H_1 scale like $1/R_2^2$, the effect of the Casimir energy becomes less important for small R_2. We have also numerically

checked that a smaller radius of the target sphere reduces the effect of the Casimir energy term significantly. For example for $R_1 = 1$ and $R_2 = \frac{1}{4}$, there is only one transposition, compared to the H_1 spectrum.

Throughout this paper we have used the convention that $\hbar = 1$. If we reinstate the parameter $\hbar$ then the classical energy scales like $\hbar^0$, the Casimir energy scales like $\hbar^1$ whereas the Laplacian and curvature terms scale like $\hbar^2$. Hence, $\hbar$ can be removed by redefining $R_1 \mapsto R_1/\hbar$, so the semi-classical limit $\hbar \to 0$ coincides (formally) with the planar limit $R_1 \to \infty$.
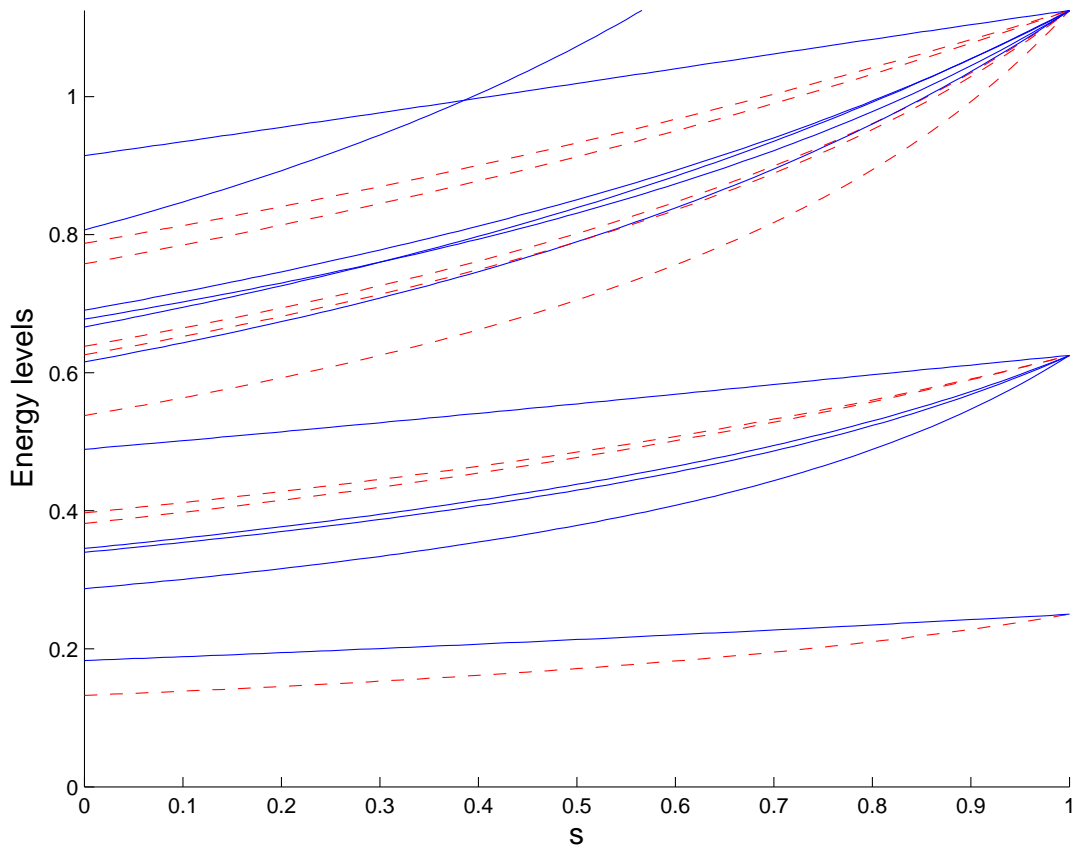

Figure 3: Energy levels interpolating between the L^2 metric and the $\mathbb{C}P^3$ metric. Here solid lines correspond to positive and dashed lines to negative parity.

5.6 Deformation to the Fubini-Study metric

As a nontrivial test of our calculations we calculate how the spectrum changes as the metric is smoothly deformed from the L^2 metric to the well-known Fubini-Study metric of $\mathbb{C}P^3$, where the spectrum and degeneracy of the Laplace operator have been calculated explicitly. We consider the one-parameter family of $SO(3) \times SO(3)$ invariant kähler metrics defined, as in

Proposition 1, by the functions

$$A_s(\lambda) = 32sA_{FS}(\lambda) + (1-s)A_{L^2}(\lambda), \qquad 0 \le s \le 1, \tag{5.27}$$

where A_{FS} and A_{L^2} are given in (2.14) and (2.12), respectively, and the factor of 32 ensures that the eigenvalues of the two Laplacians are of the same order of magnitude. The pth eigenvalue of the Laplacian for the Fubini-Study metric on $\mathbb{C}P^3$ with constant holomorphic sectional curvature 4 (and hence coefficient function A_{FS}) is

$$E_p = 4p(3+p) \tag{5.28}$$

with degeneracy

$$\deg(E_p) = \tfrac{3}{4}(3+2p)(p+1)^2(p+2)^2, \tag{5.29}$$

for $p \ge 1$ [6]. Although it is not made clear in [6], the degeneracy of $E_0 = 0$ must be 1 by the Hodge isomorphism theorem, since $\mathbb{C}P^3$ is connected, hence $\dim H^0(\mathbb{C}P^3) = 1$ which equals the dimension of the space of harmonic 0-forms. Note that $\deg(E_p)$ for $p \ge 1$ is an integer divisible by 9. In figure 3 we show how the energy levels change as the parameter s in (5.27) is increased from 0 (the L^2 metric) to 1 (the Fubini-Study metric). We distinguish between states with even and odd parity. The ground state is $E_0 = 0$ for both metrics. In figure 3 we follow all the energy levels of table 1, and it can be seen how the different energy levels become degenerate at $s = 1$, the Fubini-Study limit. Our numerically computed energy levels agree with the exact result to at least two decimal places, when we take into acount the factor $\frac{1}{2}$ in H_0 and normalize the Fubini-Study energy by a factor of 32, which arises from the factor 32 in (5.27).

Our numerical scheme at $s = 1$ does not find all eigenfunctions of $\triangle$ on $\mathbb{C}P^3$, because, except for the ground state, we impose a boundary condition which forces the wavefunction to vanish on $\partial_\infty \mathsf{Rat}_1$, the boundary of Rat_1 at infinity. It is known [37] that $\partial_\infty \mathsf{Rat}_1$ coincides with the image of the inclusion $\mathbb{C}P^1 \times \mathbb{C}P^1 \hookrightarrow \mathbb{C}P^3$, $([a_0,a_1],[b_0,b_1]) \mapsto [a_0b_1, a_1b_1, a_1b_1, a_1b_0]$. The stabilizer of this subset of $\mathbb{C}P^3$ in $SU(4)$, the isometry group of $\mathbb{C}P^3$, is isomorphic to $SU(2) \times SU(2)$ (the isometry group of Rat_1 itself). So, given an eigenfunction vanishing on $\partial_\infty \mathsf{Rat}_1$, the $SU(4)$ action generates a 9-dimensional orbit of degenerate eigenfunctions which do not vanish on $\partial_\infty \mathsf{Rat}_1$ (because $\dim SU(4) = 15$ and $\dim SU(2) \times SU(2) = 6$). Hence, we expect the degeneracies found by our numerics (at $s = 1$) to be a factor 9 smaller than the degeneracies of the true Laplacian on $\mathbb{C}P^3$. This is precisely what we find in our numerics. For example, the degeneracy of the second $\mathbb{C}P^3$ eigenvalue is $\deg(E_1)/9 = 15$, which corresponds to the levels $\{0,1\}$ and $\{1,1\}$ with degeneracy $2*3 + 3*3 = 15$, see table 1. Similarly, $\deg(E_2)/9 = 84$, corresponds to $\{0,0\}$, $\{1,1\}$, $\{0,2\}$, $\{1,1\}$, $\{1,2\}$, and $\{2,2\}$ with $1 + 3*3 + 2*5 + 3*3 + 2*3*5 + 5*5 = 84$. Further, $\deg(E_3)/9 = 300$, which corresponds to $\{0,1\}$, $\{1,1\}$, $\{1,2\}$, $\{0,3\}$, $\{1,2\}$, $\{2,2\}$, $\{1,3\}$, $\{2,2\}$, $\{2,3\}$, and $\{3,3\}$, whose degenercies add up to 300, as expected. To display all the levels which contribute to the fourth energy eigenvalue of $\mathbb{C}P^3$ we have also included the $\{3,3\}$ level in figure 3. Note that the second excited $\{0,0\}$ state contributes to the fifth energy eigenvalue of $\mathbb{C}P^3$.

6 Concluding remarks

In this paper we discussed the semi-classical quantization of soliton dynamics for $\mathbb{C}P^1$ lumps moving on a 2-sphere. We followed Moss and Shiiki [28] who derived a Born-Oppenheimer approximation to the quantum dynamics based on the moduli space approximation. We were able to evaluate three different truncations of the Born-Oppenheimer Hamiltonian H_{BO}, namely the geometric Laplacian $H_0 = \frac{1}{2}\triangle$, the first geometric correction H_1 given by the scalar curvature κ of the moduli space, and the Hamiltonian H_2 which consists of H_1 together with the Casimir energy. The Casimir energy is notoriously difficult to evaluate. At $\lambda = 0$ and $\lambda = \infty$ the spectrum of the Jacobi operator is known explicitly. Our approach is to calculate the regularized Casimir energy using zeta-function regularization for $\lambda = 0$ and $\lambda = \infty$. Then the intermediate values are calculated using an approximate self-similarity of the eigenvalue spectrum. We calculated the first 19 energy levels for H_0, H_1 and H_2, and found that the first two spectra are remarkably similar whereas the inclusion of the Casimir energy leads to significant changes. There is an overall shift of the spectrum of H_1 and H_2. The relative errors between H_0 and H_1 are 15% for the first excited state and less that 8% for other excited states. By contrast, the relative errors between H_0 and H_2 are as high as 24% for some excited states. There are only two transpositions of states where energy levels of H_1 do not have the same order compared to the H_0 spectrum. However, the spectrum of H_2 shows many transpositions.

We proved that all the spectra enjoy a rather surprising spin-isospin exchange symmetry. The proof rested on the identification of a hidden isometry of Rat_1 which becomes manifest only after one identifies $\mathsf{Rat}_1 \cong TSO(3)$. As a non-trivial check of our calculations we calculated how the energy levels change when we interpolate between the L^2 metric and the Fubini-Study metric on $\mathbb{C}P^3$. We reproduced the known spectrum for $\mathbb{C}P^3$ and discussed the degeneracies of the energy levels.

Our approach allows us to calculate the spectrum of the Laplacian for any $SO(3) \times SO(3)$ invariant kähler metric on Rat_1. One interesting choice is $A = c/\Lambda$, for which the coefficient of $(\boldsymbol{\lambda} \cdot \mathbf{T})^2$ vanishes in (5.1). In this case, the angular momentum operator $\mathbf{L}^2$ also commutes with the Hamiltonian and l becomes an additional quantum number.

The lump dynamics serves as a toy model for other solitons. For example in three spatial dimensions, two physically relevant models are the Skyrme model [34] and the Faddeev-Hopf model [10, 11]. In both models, the solitons can be quantized as fermions due to so-called Finkelstein-Rubinstein constraints [12]. Adkins, Nappi and Witten first quantized the $B = 1$ Skyrmion in [2]. The effects of the Casimir energy on the predictions of the Skyrme model in the $B = 1$ sector have been discussed in great detail in [26]. The authors calculated the 1-loop corrections to various physical quantities using phase-shift techniques to evaluate the Casimir energy. For higher topological charge the ground and lowest excited states in the Skyrme model and the Faddeev-Hopf model were calculated in [15, 18, 4] and [19] using zero-mode quantization and Finkelstein-Rubinstein constraints. The results of this paper suggest that the order of the states would remain the same, with minor changes, if the curvature correction in the Born-Oppenheimer approximation was taken into account. However, the Casimir energy could lead to significant changes in the order of states. A more careful analysis of higher order terms in these models, and in particular, of the Casimir energy, would be very useful.

Acknowledgments

Appendix

A   The rough Laplacian

In this appendix we will compute in detail the action of the rough Laplacian $\triangle_\varphi$ on sections Y of $\varphi^{-1}TN$ of the form

$$Y = a(\theta) \cos m\phi \widetilde{E}_1. \tag{A.1}$$

Recall that $(M, g) = (N, h) = $ the unit sphere, (θ, ϕ) are the usual polar coordinates on M or N, $E_1 = \partial/\partial\theta$, $E_2 = \operatorname{cosec}\theta \partial/\partial\phi$ is an orthonormal frame on M or N, $\widetilde{E}_1 = E_1 \circ \varphi$, $\widetilde{E}_2 \circ \varphi$, and $\varphi : M \to N$ is a map of the form $\varphi(\theta, \phi) = (f(\theta), \phi)$ in polar coordinates. Now, given a map between Riemannian manifolds $\varphi : M \to N$, the pullback connexion ∇^φ is the unique connexion on the vector bundle $\varphi^{-1}TN$ satisfying the axioms

$$\nabla_X^\varphi(Y_1 + Y_2) = \nabla_X^\varphi Y_1 + \nabla_X^\varphi Y_2 \tag{A.2}$$

$$\nabla_X^\varphi(fY_1) = X[f]Y_1 + f\nabla_X^\varphi Y_1 \tag{A.3}$$

$$\nabla_X^\varphi(Y \circ \varphi) = (\nabla_{\mathrm{d}\varphi X}^N Y) \circ \varphi \tag{A.4}$$

for all $X \in \Gamma(TM)$, $Y_1, Y_2 \in \Gamma(\varphi^{-1}TN)$, $f \in C^\infty(M)$ and $Y \in \Gamma(TN)$, where ∇^N is the Levi-Civita connexion on (N, h). In our case ∇^N (which coincides with ∇^M) is determined by its action on the frame $\{E_1, E_2\}$,

$$\nabla^N E_1 = \cot\theta \, e_2 \otimes E_2, \qquad \nabla^N E_2 = -\cot\theta \, e_2 \otimes E_1, \tag{A.5}$$

where $\{e_1, e_2\}$ is the coframe dual to $\{E_1, E_2\}$. From this we may deduce how ∇^φ acts on $\widetilde{E}_1, \widetilde{E}_2$. By property (A.4) and (A.5),

$$\nabla_{E_1}^\varphi \widetilde{E}_1 = (\nabla_{f'(\theta)E_1}^N E_1) \circ \varphi = 0 \tag{A.6}$$

$$\nabla_{E_1}^\varphi \widetilde{E}_2 = (\nabla_{f'(\theta)E_1}^N E_2) \circ \varphi = 0 \tag{A.7}$$

$$\nabla_{E_2}^\varphi \widetilde{E}_1 = (\nabla_{\frac{\sin f}{\sin\theta}E_2}^N E_1) \circ \varphi = \frac{\cos f}{\sin\theta}\widetilde{E}_2 \tag{A.8}$$

$$\nabla_{E_2}^\varphi \widetilde{E}_2 = (\nabla_{\frac{\sin f}{\sin\theta}E_2}^N E_2) \circ \varphi = -\frac{\cos f}{\sin\theta}\widetilde{E}_1. \tag{A.9}$$

The rough Laplacian has 4 terms,

$$\triangle_\varphi Y = -\nabla_{E_1}^\varphi(\nabla_{E_1}^\varphi Y) - \nabla_{E_2}^\varphi(\nabla_{E_2}^\varphi Y) + \nabla_{\nabla_{E_1}^M E_1}^\varphi Y + \nabla_{\nabla_{E_2}^M E_2}^\varphi Y. \tag{A.10}$$

We evaluate these in turn, for $Y = a(\theta) \cos m\phi \widetilde{E}_1$. First

$$\nabla^\varphi_{E_1} (\nabla^\varphi_{E_1} a \cos m\phi \widetilde{E}_1) = \frac{\partial^2}{\partial \theta^2} (a \cos m\phi) \widetilde{E}_1 = a'' \cos m\phi \widetilde{E}_1. \tag{A.11}$$

The second term is more involved:

$$
\begin{aligned}
\nabla^\varphi_{E_2} (a \cos m\phi \widetilde{E}_1) &= a E_2 [\cos m\phi] \widetilde{E}_1 + a \cos m\phi \nabla^\varphi_{E_2} \widetilde{E}_1 \\
&= -ma \frac{\sin m\phi}{\sin \theta} \widetilde{E}_1 + a \frac{\cos m\phi \cos f}{\sin \theta} \widetilde{E}_2 \tag{A.12} \\
\Rightarrow \nabla^\varphi_{E_2} (\nabla^\varphi_{E_2} a \cos m\phi \widetilde{E}_1) &= -m^2 a \frac{\cos m\phi}{\sin^2 \theta} \widetilde{E}_1 - 2ma \frac{\sin m\phi \cos f}{\sin^2 \theta} \widetilde{E}_2 \\
&\quad - a \frac{\cos m\phi \cos^2 f}{\sin^2 \theta} \widetilde{E}_1. \tag{A.13}
\end{aligned}
$$

The third term vanishes since $\nabla^M_{E_1} E_1 = 0$, while the fourth term is

$$\nabla^\varphi_{\nabla^M_{E_2} E_2} (a \cos m\phi \widetilde{E}_1) = - \cot \theta \nabla^\varphi_{E_1} (a \cos m\phi \widetilde{E}_1) = -a' \cot \theta \cos m\phi \widetilde{E}_1. \tag{A.14}$$

Assembling the pieces, one sees that

$$
\begin{aligned}
\triangle_\varphi (a \cos m\phi \widetilde{E}_1) &= \left(-a'' - a' \cot \theta + \frac{m^2}{\sin^2 \theta} a + \frac{\cos^2 f}{\sin^2 \theta} a \right) \cos m\phi \widetilde{E}_1 \\
&\quad + \left(\frac{2m \cos f}{\sin^2 \theta} a \right) \sin m\phi \widetilde{E}_2, \tag{A.15}
\end{aligned}
$$

as claimed in equation (4.14).

B Angular momentum calculations

In this appendix we briefly describe the evaluation of the operator $(\boldsymbol{\lambda} \cdot \mathbf{T})^2$. We closely follow the notation in [8]. Note the spin quantum number j satisfies $j = k$ since $\mathbf{J}^2 = \mathbf{K}^2$. We choose the following convention for the spherical harmonics,

$$Y_{l,m}(\theta, \phi) = (-1)^m \sqrt{\frac{(2l+1)}{4\pi} \frac{(l-m)!}{(l+m)!}} P_l^m(x) \exp(im\phi), \tag{B.16}$$

where the associated Legendre polynomials are given by

$$P_l^m(x) = \frac{(1-x^2)^{m/2}}{2^l l!} \frac{d^{l+m}}{dx^{l+m}} (x^2 - 1)^l. \tag{B.17}$$

Note that $Y^*_{l,m} = (-1)^m Y_{l,-m}$ and

$$\int_0^{2\pi} \int_0^\pi Y^*_{l,m}(\theta, \phi) Y_{l',m'}(\theta, \phi) \sin \theta \, d\theta d\phi = \delta_{ll'} \delta_{mm'}. \tag{B.18}$$

It is easy to show that $(\boldsymbol{\lambda} \cdot \mathbf{T}) = (\boldsymbol{\lambda} \cdot \mathbf{J})$, and we showed in section 3 that this operator commutes with $\mathbf{T}$ and $\mathbf{J}^2$. Hence, the operator does not change the quantum numbers t, k, k_3 and t_3. Furthermore, the matrix elements are independent of t_3 and k_3, hence we can choose without loss of generality $t_3 = 0$ and $k_3 = 0$. We need to evaluate

$$M \equiv (M_{\tilde{l}l}) = \langle k, \tilde{l}, t, 0 | \boldsymbol{\lambda} \cdot \mathbf{J} | k, l, t, 0 \rangle, \tag{B.19}$$

which is a $(2 \min(k,t)+1)$ by $(2 \min(k,t)+1)$ matrix, because the angular momentum quantum numbers satisfy $\min(k,t) \leq l, \tilde{l} \leq k+t$. Since $\boldsymbol{\lambda} \cdot \mathbf{J}$ is a Hermitian operator the matrix M is Hermitian, namely

$$M_{\tilde{l}l} = M_{l\tilde{l}}^{\dagger}. \tag{B.20}$$

Using Clebsch-Gordan coefficients (B.19) can be rewritten as

$$M = \sum_{m_1, m_2} (k, \tilde{l}, t, 0 | k, m_1, \tilde{l}, -m_1) \langle k, m_1, \tilde{l}, -m_1 | \boldsymbol{\lambda} \cdot \mathbf{J} | k, m_2, l, -m_2 \rangle (k, m_2, l, -m_2 | k, l, t, 0).$$
$$\tag{B.21}$$

The operator $\boldsymbol{\lambda} \cdot \mathbf{J}$ can be written in terms of spherical harmonics as

$$\boldsymbol{\lambda} \cdot \mathbf{J} = \frac{2\sqrt{\pi}\lambda}{\sqrt{3}} \left(-\frac{1}{\sqrt{2}} Y_{1,1} J_- + \frac{1}{\sqrt{2}} Y_{1,-1} J_+ + Y_{1,0} J_3 \right). \tag{B.22}$$

Hence, we only need to evaluate

$$\langle k, m_1 | J_+ | k, m_2 \rangle = \delta_{m_1, m_2+1} \sqrt{(k-m_2)(k+m_2+1)}, \tag{B.23}$$
$$\langle k, m_1 | J_- | k, m_2 \rangle = \delta_{m_1, m_2-1} \sqrt{(k+m_2)(k-m_2+1)}, \tag{B.24}$$
$$\langle k, m_1 | J_3 | k, m_2 \rangle = \delta_{m_1, m_2} m_2, \tag{B.25}$$

and

$$\langle \tilde{l}, m_1 | Y_{l,m} | l, m_2 \rangle, \tag{B.26}$$

which can be calculated using (4.6.3) in [8], namely,

$$\int_0^{2\pi} \int_0^{\pi} Y_{l_1,m_1}(\theta, \phi) Y_{l_2,m_2}(\theta, \phi) Y_{l_3,m_3}(\theta, \phi) \sin\theta \mathrm{d}\theta \mathrm{d}\phi \tag{B.27}$$

$$= \sqrt{\frac{(2l_1+1)(2l_2+1)(2l_3+1)}{4\pi}} \begin{pmatrix} l_1 & l_2 & l_3 \\ 0 & 0 & 0 \end{pmatrix} \begin{pmatrix} l_1 & l_2 & l_3 \\ m_1 & m_2 & m_3 \end{pmatrix}, \tag{B.28}$$

where the two matrices in (B.28) correspond to $3j$ symbols. The $3j$ symbol

$$\begin{pmatrix} \tilde{l} & l & 1 \\ 0 & 0 & 0 \end{pmatrix} \tag{B.29}$$

vanishes unless $\tilde{l} = l \pm 1$, which can be used to show that M vanishes in the cases $k = 0$ or $t = 0$. For example, for $k = 0$ the only allowed values of the angular momentum are $l = t$ and $\tilde{l} = t$, which vanishes since $\tilde{l} \neq l \pm 1$.

Following the notation in [8], the Clebsch-Gordan coefficients and the $3j$ symbols have real entries. Hence, M is a real matrix and (B.20) implies that M is symmetric. Note that the eigenvalues of M are $0, \pm 1, \pm 2, \ldots, \pm \min(k,t)$, which can be explained as follows. Heuristically, $(\boldsymbol{\lambda} \cdot \mathbf{T})$ is the projection of the total angular momentum operator onto the $\boldsymbol{\lambda}$ direction. Hence, it can be rotated by a change of variables to T_3 which has eigenvalues $0, \pm 1, \cdots \pm \min(k,t)$. The highest possible value of t_3 is $\min(k,t)$ because the dimension of M is $2\min(k,t) + 1$.

Now, we can evaluate the matrix (B.19) for various values of k and t using Maple, for example. For small values the formulae are more tractable. For example for $(k,t) = (1,t)$ we obtain

$$M^2 = \langle 1, \tilde{l}, t, 0 | (\boldsymbol{\lambda} \cdot \mathbf{J})^2 | 1, l, t, 0 \rangle = \frac{\lambda^2}{2t+1} \begin{pmatrix} t+1 & 0 & \sqrt{t(t+1)} \\ 0 & 2t+1 & 0 \\ \sqrt{t(t+1)} & 0 & t \end{pmatrix}. \qquad \text{(B.30)}$$

We showed in section 5.1 that there is a $(k,t) \to (t,k)$ for the respective matrices M. This was verified by explicit calculation for all values (k,t) in table 1. As can be seen in (B.30) there is a natural chess board structure in the matrix M^2, which follows from the fact that M vanishes unless $\tilde{l} = l \pm 1$, and hence M^2 vanishes unless $\tilde{l} = l+2$, l, or $l-2$.

References

[1] M. Abramowitz and I. A. Stegun, *Handbook of Mathematical Functions* (Dover Publications, tenth edition, 1972).

[2] G. S. Adkins, C. R. Nappi and E. Witten, "Static Properties of Nucleons in the Skyrme Model," Nucl. Phys. B **228** (1983) 552-584.

[3] J.M. Baptista, "Some special Kähler metrics on $SL(2, \mathbb{C})$ and their holomorphic quantization" *J. Geom. Phys.* **50** (2004) 1-27.

[4] R. A. Battye, N. S. Manton, P. M. Sutcliffe and S. W. Wood, "Light Nuclei of Even Mass Number in the Skyrme Model," Phys. Rev. C **80** (2009) 034323-034338.

[5] A.L. Besse, *Einstein Manifolds* (Springer-Verlag, Berlin, Germany, 2002).

[6] M. Berger, P. Gauduchon, E. Mazet, *Le Spectre d'une Variété Riemannienne* (Springer-Verlag, 1971).

[7] P. Bizon, T. Chmaj and Z. Tabor, "Formation of singularities for equivariant $(2+1)$-dimensional wave maps into the 2-sphere" *Nonlinearity* **14** (2001) 1041-53.

[8] E.R. Edmonds, *Angular Momentum in Quantum Mechanics* (Princeton University Press, Princeton, New Jersey, 1960).

[9] E. Elizalde, S.D. Odintsov, A. Romeo, A.A. Bytsenko and S. Zerbini, *Zeta Regularization Techniques with Applications* (World Scientifique, Singapore, 1994).

[10] L. D. Faddeev, "Quantisation of solitons" (Preprint IAS Print-75-QS70, Princeton, 1975).

[11] L. D. Faddeev and A. J. Niemi, "Knots and particles" *Nature* **387** (1997) 58-61.

[12] D. Finkelstein and J. Rubinstein, "Connection between spin, statistics, and kinks" *J. Math. Phys.* **9** (1968) 1762-1779.

[13] G.W. Gibbons and N.S. Manton, "Classical and quantum dynamics of BPS monopoles" *Nucl. Phys.* **B274** (1986) 183-224.

[14] M. Haskins and J.M. Speight, "The geodesic approximation for lump dynamics and coercivity of the Hessian for harmonic maps" *J. Math. Phys.* **44** (2003) 3470-94.

[15] P. Irwin, "Zero mode quantization of multi - Skyrmions," Phys. Rev. D **61** (2000) 114024-114057.

[16] A.W. Knapp, *Representation Theory of Semisimple Groups*, (Princeton University Press, Princeton NJ, USA, 1986), p17.

[17] S. Kobayashi and K. Nomizu, *Foundations of Differential Geometry* (John Wiley, New York, USA, 1996) Volume II, p167.

[18] S. Krusch, "Homotopy of rational maps and the quantization of skyrmions" *Annals Phys.* **304** (2003) 103-127.

[19] S. Krusch and J.M. Speight, "Fermionic quantization of Hopf solitons" *Commun. Math. Phys.* **264** (2006) 391-410.

[20] A. Lichnerowicz, "Applications harmoniques et variétés kähleriennes" *Symp. Math. Bologna* **3** (1970) 341-402.

[21] J.M. Linhart and L.A. Sadun, "Fast and slow blowup in the S^2 σ model and the $(4+1)$-dimensional Yang-Mills model" *Nonlinearity* **15** (2002) 219-238.

[22] N.S. Manton, "A remark on the scattering of BPS monopoles" *Phys. Lett.* **110B** (1982) 54-56.

[23] N.S. Manton and P.M. Sutcliffe, *Topological Solitons* (Cambridge University Press, Cambridge, UK, 2004).

[24] J.A. McGlade, *The Dynamics of Topological Solitons within the Geodesic Approximation* (PhD Thesis, University of Leeds, 2005).

[25] J.A. McGlade and J.M. Speight, "Slow equivariant lump dynamics on the two-sphere" *Nonlinearity* **19** (2006) 441-452.

[26] F. Meier and H. Walliser, "Quantum Corrections to Baryon Properties in Chiral Soliton Models," Phys. Rept. **289** (1997) 383-448.

[27] I.G. Moss, "Soliton vacuum energies and the CP(1) model" *Phys. Lett.* **B460** (1999) 103-106.

[28] I.G. Moss and N. Shiiki, "Quantum mechanics on moduli spaces" *Nucl. Phys.* **B565** (2000) 345-362.

[29] I. G. Moss, N. Shiiki and T. Torii, "Vacuum energy of CP(1) solitons," (Preprint: arXiv:hep-ph/0103240, 2001).

[30] J.D. Pryce, *Numerical Solution of Sturm-Liouville Problems* (Oxford University Press, Oxford, UK, 1993).

[31] I. Rodnianski and J. Sterbenz, "On the Formation of Singularities in the Critical $O(3)$ Sigma-Model" *Ann. Math.* **172** (2010) 187-242.

[32] P.J. Ruback, "Sigma model solitons and their moduli space metrics" *Commun. Math. Phys.* **116** 645-58.

[33] L. Sadun and J.M. Speight, "Geodesic incompleteness in the $\mathbb{C}P^1$ model on a compact Riemann surface" *Lett. Math. Phys.* **43** (1998) 329-34.

[34] T. H. R. Skyrme, "A nonlinear field theory" *Proc. Roy. Soc. Lond.* **A260** (1961) 127-138.

[35] R.T. Smith, "The second variation formula for harmonic mappings" *Proc. Amer. Math. Soc.* **47** (1975) 229-36.

[36] J.M. Speight, "Low energy dynamics of a $\mathbb{C}P^1$ lump on the sphere" *J. Math. Phys.* **36** (1995) 796-813.

[37] J.M. Speight, "The L^2 geometry of spaces of harmonic maps $S^2 \to S^2$ and $\mathbb{R}P^2 \to \mathbb{R}P^2$" *J. Geom. Phys.* **47** (2003) 343-368.

[38] D. Stuart, "Dynamics of abelian Higgs vortices in the near Bogomolny regime" *Commun. Math. Phys.* **159** (1994) 51-91.

[39] D. Stuart, "The geodesic approximation for the Yang-Mills-Higgs equations" *Commun. Math. Phys.* **166** (1994) 149-90.

[40] H. Urakawa, *Calculus of Variations and Harmonic Maps* (American Mathematical Society, Providence RI, USA, 1993).

[41] T.J. Willmore, *Riemannian Geometry* (Clarendon Press, Oxford, UK, 1993) p57.